Mineralogy and geochemistry of platinum-rich chromitites from the mantle-crust transition zone at Ouen Island, New Caledonia ophiolite

José María Gonzalez-Jimenez, Thierry Auge, Fernando Gervilla, Laurent Bailly, Joaquin A. Proenza, William L. Griffin

MINERALOGY AND GEOCHEMISTRY OF PLATINUM-RICH CHROMITITES FROM THE MANTLE–CRUST TRANSITION ZONE AT OUEN ISLAND, NEW CALEDONIA OPHIOLITE

JOSÉ MARÍA GONZÁLEZ-JIMÉNEZ[§]

ARC Centre of Excellence for Core to Crust Fluid Systems (CCFS) and GEMOC National Key Centre, Department of Earth and Planetary Sciences, Macquarie University, Sydney NSW 2109, Australia

THIERRY AUGÉ

BRGM (Bureau de Recherches Géologiques et Minières), Mineral Resources Division, 3, avenue Claude-Guillemin, B.P. 36009, F–45060 Orleans, France

FERNANDO GERVILLA

Departamento de Mineralogía y Petrología, and Instituto Andaluz de Ciencias de la Tierra (Universidad de Granada – CSIC), Avda. Fuentenueva s/n, E–18002 Granada, Spain

LAURENT BAILLY

BRGM (Bureau de Recherches Géologiques et Minières), Mineral Resources Division, 3, avenue Claude-Guillemin, B.P. 36009, F–45060 Orléans, France

JOAQUIN A. PROENZA

Departament de Cristal·lografia, Mineralogia i Dipòsits Minerals, Facultat de Geologia, Universitat de Barcelona, Martí i Franquès s/n, E–08028 Barcelona, Spain

WILLIAM L. GRIFFIN

ARC Centre of Excellence for Core to Crust Fluid Systems (CCFS) and GEMOC National Key Centre, Department of Earth and Planetary Sciences, Macquarie University, Sydney NSW 2109, Australia

ABSTRACT

Micropods, irregular bodies and schlieren of chromitite occur within a unit of layered plagioclase-bearing wehrlite on Ouen Island, southern New Caledonia. The primary chromian spinel is Al-rich, with Cr# [atomic (Cr/Cr + Al)] between 0.52 and 0.62, and Mg# [Mg/(Mg + Fe^{2+})] between 0.57 and 0.72. Contents of minor and trace elements (Ga, Ni, Zn, Co, Mn, V, Sc) in primary spinel, obtained by LA–ICP–MS, are comparable to those reported in chromian spinel from podiform chromitites in other ophiolite complexes. The chromitites are strongly enriched in Pt and Pd (up to 11.5 ppm Pt + Pd), reflecting the presence of abundant platinum-group minerals (PGM), including alloys, sulfides, oxides and compounds containing Te, Sb or Hg. Also present are Ru–(Os–Ir) phases, in accessory amounts: sulfides (mainly laurite, two unidentified Os–S and Ir–S compounds) and sulfarsenides of Ir and Rh. Abundant base-metal minerals (BMM) occur together with the PGM; they include Ni–Cu–Fe sulfides (pentlandite, millerite, heazlewoodite, chalcopyrite and bornite), awaruite (Ni_3Fe), and a phase with a composition close to NiAsS (probably gersdorffite). The geochemistry and mineralogy of the chromitite and the PGE mineralization show that the Ouen Island chromitites have a different origin than those found in the mantle and crust sequences of the New Caledonia ophiolite complex. The distribution, morphology and composition of the PGM and BMM in the chromitites define two distinct paragenetic assemblages: i) primary or magmatic, consisting of PGM and BMS grains enclosed in the unaltered core of chromian spinel grains and in primary anhydrous silicates (olivine and pyroxene) of the matrix; ii) secondary or postmagmatic, consisting of PGM and BMM grains found along fractures, enclosed or in contact with high-temperature secondary hydrous silicates

§ *E-mail address*: jose.gonzalez@mq.edu.au

(amphibole) and low-temperature silicates (serpentine, chlorite). Microtextural and compositional data for the secondary PGM and BMM mineral assemblages suggest that after the crystallization of chromian spinel, an excess of H_2O generated a residual high-temperature hydrothermal fluid that modified the magmatic PGM mineralogy, producing small-scale remobilization of the PGE. Late serpentinization overprinted this hydrothermal alteration, and contributed to the degradation of the primary PGM and BMM. At this stage, PGE-bearing alloys and sulfides were replaced by new stable alloys and oxides of the PGE.

Keywords: chromitites, platinum, palladium, platinum-group minerals, mantle–crust transition zone, New Caledonia Ophiolite, Ouen Island.

Sommaire

Des chromitites, sous forme de micro-pods, de corps irréguliers et de schlieren, se trouvent dans une unité de wehrlite à plagioclase litée sur l'île d'Ouen, située au sud de la Nouvelle-Calédonie. La chromite primaire est riche en Al, avec Cr# [(Cr/Cr + Al)] entre 0.52 et 0.62, et Mg# [Mg/(Mg + Fe^{2+})] entre 0.57 et 0.72. Les teneurs en éléments mineurs et en traces (Ga, Ni, Zn, Co, Mn, V, Sc) de ces spinelles, obtenues par ICP–MS ablation laser, sont comparables à celles de spinelles chromifères de chromitites podiformes d'autres complexes ophiolitiques. Ces chromitites sont fortement enrichies en Pt et Pd (jusqu'à 11,5 ppm Pt + Pd), traduisant l'abondance de minéraux du groupe du platine (MGP), sous forme d'alliages, de sulfures, d'oxydes et de minéraux à Te, Sb ou Hg. Des minéraux porteurs de Ru–(Os–Ir) sont aussi présents mais plus rares, sous forme de sulfures (laurite principalement, et des composés Os–S et Ir–S non identifiés), et de sulfo-arséniures d'Ir et Rh. Avec les MGP se trouvent d'abondants minéraux de métaux de base (MMB); ce sont soit des sulfures de Ni–Cu–Fe (pentlandite, millerite, heazlewoodite, chalcopyrite et bornite), de l'awaruite (Ni_3Fe) et un composé de composition proche de NiAsS (probablement gersdorffite). La composition chimique et la minéralogie des chromitites, ainsi que la minéralisation en éléments du groupe du platine (EGP), indiquent que les chromitites de l'île Ouen ont une origine différente de celle des chromitites des séquences mantelliques et crustales du complexe ophiolitique de Nouvelle-Calédonie. La distribution, la morphologie et la composition des MGP et des MMB dans les chromitites définissent deux associations paragénétiques: 1) une association primaire, magmatique, avec des MGP et des MMB inclus dans le cœur non altéré des grains de spinelle chromifère et dans les silicates primaires (olivine et pyroxène) de la matrice, et 2) une association secondaire ou post-magmatique, avec des MGP et des MMB disposés le long de fractures, inclus ou en contact avec des silicates secondaires hydroxylés de haute température (amphibole) et des silicates de basse température (serpentine, chlorite). Les relations microtexturales et les compositions de la paragenèse secondaire à MGP et MMB suggèrent qu'après la cristallisation du spinelle chromifère, un excès de H_2O a généré un fluide hydrothermal résiduel de haute température, qui a modifié la minéralogie des MGP magmatiques, produisant une remobilisation locale des EGP. La serpentinisation s'est ensuite superposée à cette altération hydrothermale, et a contribué à la déstabilisation des MGP et des MMB primaires, provoquant le remplacement des alliages et sulfures des EGP en de nouvelles espèces stables d'alliages et d'oxydes d'EGP.

Mots-clés: chromitites, platine, palladium, minéraux du groupe du platine, transition manteau–croûte, ophiolite, île Ouen, Nouvelle-Calédonie.

Introduction

The New Caledonia Ophiolite has a bimodal distribution of chromite mineralization: i) *podiform chromitites* hosted in mantle dunite–harzburgite (*e.g.*, Massif du Sud, Tiébaghi and Poum), and ii) *stratiform* or *banded* chromitites located in cumulates formed in the lower crust (*e.g.*, Pirogues). These two types of chromitites display distinctly different geochemistry and mineralogy of platinum-group elements (PGE). Podiform chromitites are enriched in refractory PGE (*i.e.*, Ir, Os, Ru); they contain abundant minerals of the laurite (RuS_2) – erlichmanite (OsS_2) solid-solution series and Os–Ir alloy (Legendre & Augé 1986, Augé 1988, Augé & Johan 1988, Augé *et al.* 1998). In contrast, banded chromitites preferentially concentrate incompatible PGE (Pt, Pd, Rh), and have a PGM mineralogy dominated by minerals of the system Pt–Fe–(Cu) (primary alloys and secondary oxides), and less abundant Pt-rich sulfides containing Ni, Cu and Fe (*e.g.*, Augé & Legendre 1994, Augé & Maurizot 1995, Augé *et al.* 1998). The origin of both types of chromitites, and their distinctly different PGE geochemistry and mineralogy, have been interpreted as a result of the crystallization of mantle-derived melts (with different degrees of fractionation, fO_2 and fS_2) that were emplaced at different levels of the ophiolitic section (*e.g.*, Augé 1988, Augé & Johan 1988, Augé & Maurizot 1995). Postmagmatic processes, such as subaerial weathering (*i.e.*, laterization), have also been considered to play an important role in modifying the primary PGM assemblages, and in the small-scale remobilization of PGE (*e.g.*, Augé & Legendre 1994).

In this paper, we provide the first description of chromitites associated with the mantle–crust transition zone of the New Caledonia ophiolite, and present data on the composition (major and minor elements) of chromian spinel, and on the geochemistry and mineralogy of the associated PGE mineralization. A comparative study of the PGM and BMM assemblages, based on the composition and microtextural setting, has been carried

out in order to constrain the magmatic genesis of the PGE mineralization and its postmagmatic evolution.

Geological Setting

New Caledonia is a NW–SE elongate island located in the southwestern Pacific region between the New Hebrides Arc and the eastern margin of Australia (Fig. 1). A complicated tectonic history since the Late Cretaceous has involved successive openings of marginal basins (*e.g.*, Tasman Sea, New Caledonia and Loyalty basins) and the formation of island arcs, isolated microcontinental ribbons of Paleozoic–Jurassic age, and accreted terranes of the eastern Australian margin of Gondwanaland (*e.g.*, Lord Howe Rise and Norfolk Ridge; Auzende *et al.* 2000, Crawford *et al.* 2003). Late Eocene arc–microcontinent collision (~52–48 Ma) resulted in the emplacement of several portions of the Cretaceous oceanic lithosphere (100–77 Ma) on the emerged basement of the Norfolk Ridge (Prinzhofer *et al.* 1980, Prinzhofer 1981, Aitchinson *et al.* 1995, *et al.* 1998, 2001, Spandler *et al.* 2005). Post-orogenic collapse during Oligocene time (~ 27 Ma) resulted in the structural exhumation of the Norfolk Ridge basement as a metamorphic core complex in the northeastern part of New Caledonia (Cluzel *et al.* 1994, 1995, 2005, Aitchinson *et al.* 1995).

The ophiolitic nappe of New Caledonia covers approximately 6000 km^2 (Collot *et al.* 1987). It occurs as several widespread massifs along both east and west coasts of the island (Fig. 1). Almost all of these ophiolite outcrops are upper-mantle material (> 3000 m thick) (Collot *et al.* 1987, Cluzel *et al.* 2005). The crustal sequence is restricted to cumulate mafic rocks of the lower crust (Prinzhofer *et al.* 1980, Moutte 1982, Prinzhofer & Allègre 1985, Johan & Augé 1986, Collot *et al.* 1987), whereas the paleo-Moho is only preserved in few post-obduction grabens (Cluzel *et al.* 2005). The upper part of the ophiolite sequence (pillow basalts and sheeted dikes) is absent owing to thrust faulting or erosion during or after obduction (Collot *et al.* 1987). The ophiolite massifs have been classically grouped into three "units" (Moutte 1982): the northern, intermediate and southern massifs. The northern massifs (including the Tiébaghi Massif) mainly consist of depleted dunite-bearing harzburgite and plagioclase lherzolite, including large podiform deposits of chromite (the Tiébaghi mine produced more than 3 million tonnes of ore). The intermediate massif consists of harzburgite with minor bodies of dunite and rare small concentrations of chromite. The southern massif (Grand Massif du Sud) is composed of mantle harzgurgite with a tectonite structure, locally capped by dunite, wehrlite, rare pyroxenite and layered gabbro (Prinzhofer *et al.* 1980, Nicolas & Prinzhofer 1983, Prinzhofer & Allègre 1985). This massif contains abundant podiform bodies of chromitite hosted by mantle peridotite (*e.g.*, at the Anna-Madeleine mine) or, more rarely, small seams of chromite in the overlying dunite (*e.g.*, Pirogues mineralization) (Johan & Augé 1986, Augé & Johan 1988, Augé 1988, Augé & Maurizot 1995, Augé *et al.* 1998).

Ouen Island is the southernmost outcrop of the New Caledonia ophiolite (Fig. 1). The central to western part of the island (around Baie Tranquille) (Fig. 1) is dominated by a unit of strongly serpentinized mantle harzburgite with a tectonite structure. At its base, there is a deformation zone dominated by a tectonic mélange composed of altered gabbros widely distributed within a serpentine-rich matrix. Common small intrusions and dykes of plagiogranite cross-cut this mélange. In the central to eastern part of the island, mantle harzburgite is overlain by interlayered dunite–wehrlite (with interstitial plagioclase and small pockets of pyroxenite), which grades upward to plagioclase-bearing wehrlite with gabbro intervals at the top (Fig. 1). This lithological sequence is equivalent to that exposed at Montagne des Sources in the nearby Grand Massif du Sud, which is interpreted as the mantle–crust transition zone of the New Caledonia ophiolite complex (Prinzhofer *et al.* 1980, Dupuy *et al.* 1981, Nicolas & Prinzhofer 1983, Marchesi *et al.* 2009).

Sampling and Analytical Approach

Representative samples of chromitite (n = 12) were collected from three occurrences in the central and southern parts of Ouen Island (Fig. 1). Polished blocks of these samples were investigated by optical and electron microscopy and by electron-microprobe analysis. The SEM images and preliminary qualitative identification of platinum-group minerals (PGM) and base-metal minerals (BMM) by means of EDS spectra were obtained with an environmental scanning electron microscope (ESEM) equipped with EDX detector coupled to EDAX software at the Centro Andaluz de Medio Ambiente (CEAMA) (University of Granada – Junta de Andalucía, Granada, Spain). Quantitative analyses of chromian spinel and the PGM and BMM inclusions were performed with a CAMECA SX50 electron microprobe at the MMA Service (BRGM, Orléans, France). Operating conditions were: accelerating voltage 25 kV, beam current 15–20 nA, beam diameter 2 μm, and count times of 10 s on the peak. Calibration for chromite and silicates was performed using natural and synthetic reference materials. The structural formula of chromian spinel was calculated assuming stoichiometry, following Carmichael's (1967) procedure. For PGM and BMM, the following X-ray lines were measured: $K\alpha$ for S, Fe, Ni, Co, Cu and Cr, $L\alpha$ for Ru, Rh, Pd, Os, Ir, Pt, Te and Sb, and $L\beta$ for As. The interferences Ir$L\alpha$ – Cu$K\alpha$, Ru$L\beta$ – Rh$L\alpha$, and Cu $K\beta$ – Os$L\alpha$, were corrected online. Pure metals were employed as standards for Os, Ir, Ru, Rh, Pt, Pd and Ni, as well as Cr_2O_3 for Cr, FeS_2 for Fe and S, $CuFeS_2$

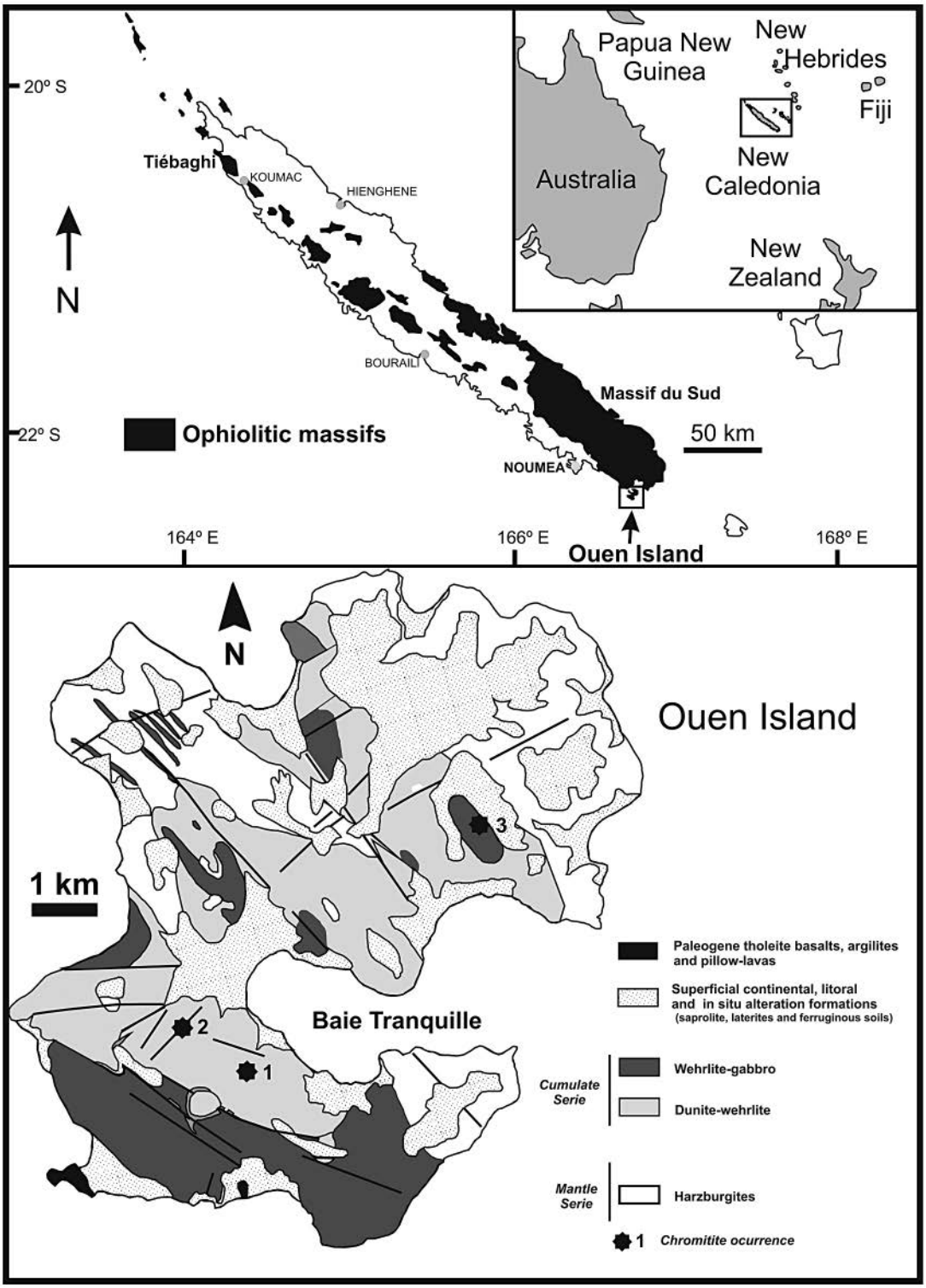
20° S
Tiébaghi
KOUMAC
HIENGHENE
N
BOURAIL
Massif du Sud
22° S
Ophiolitic massifs
50 km
NOUMEA
164° E
166° E
168° E
Ouen Island
Papua New Guinea
New Hebrides
Fiji
Australia
New Caledonia
New Zealand
N
Ouen Island
1 km
3
2
1
Baie Tranquille
Paleogene tholeite basalts, argilites and pillow-lavas
Superficial continental, litoral and in situ alteration formations (saprolite, laterites and ferruginous soils)
Cumulate Serie
Wehrlite-gabbro
Dunite-wehrlite
Mantle Serie
Harzburgites
1 Chromitite ocurrence

for Cu, GaAs for As, and Sb_2S_3 for Sb. At least two analyses were performed on each large grain of PGM and BMM to check for homogeneity and consistency. In the case of heterogeneous PGM and BMM, highly porous or less than 2 μm in size, only semiquantitative and qualitative analyses were obtained.

Concentrations of minor and trace elements in chromian spinel were established by means of LA–ICP–MS at the Geochemical Analysis Unit of GEMOC, Macquarie University, Sydney, Australia. Because minor and trace elements in chromian spinel are sensitive to subsolidus re-equilibration or hydrothermal alteration (Pagé & Barnes 2009), and both are in turn strongly dependent on the chromian spinel : silicate ratio, only grains of chromian spinel from massive chromitites (>80 vol.% chromian spinel) were selected for LA–ICP–MS analysis. We used an Agilent Technologies 7700 Series ICP–MS coupled with a UP–213 laser. The analyses were conducted using a 50-μm beam diameter, 5 Hz frequency, 5.5 mJ/pulse power, during a 180-s analysis (60 s for the gas blank and 120 s on the chromite). The external standards utilized were NIST610 and BRC2-A glasses, and the internal standard was Al_2O_3 in the chromite, which was obtained by EMP. The two external standards were analyzed twice on each single run comprising a maximum of 15 analyses in each of these runs. In addition to the minor elements sought (^{45}Sc, ^{47}Ti, ^{51}V, ^{55}Mn, ^{59}Co, ^{60}Ni, ^{66}Zn, ^{69}Ga, and ^{118}Sn), other elements (^{24}Mg, ^{27}Al, ^{42}Ca, ^{53}Cr, ^{55}Mn, ^{65}Cu, ^{72}Ge, ^{85}Rb, ^{88}Sr, ^{89}Y, ^{90}Zr, ^{93}Nb, ^{137}Ba, ^{178}Hf, ^{181}Ta, ^{182}W, ^{208}Pb, ^{232}Th) were monitored during chromite ablation, to constrain the characteristics of the ablated material and to check for the presence of included minerals. We included ^{29}Si and ^{103}Rh to evaluate the presence of silicates and PGM, respectively.

Whole-rock Pt and Pd contents were determined in chromitite samples by fire assay and ICP–MS finish. Analyses were performed at the SGS Minerals Services Laboratories, Lakefield, Ontario, Canada.

The Ouen Island Chromitites

Field relations and petrography

The Ouen Island chromitites occur as single small pods, irregular bodies or schlieren (up to 1 m long and less than 0.5 m thick) within layered plagioclase-bearing wehrlite (Figs. 2A–C) or, less commonly, as small concentrations of chromian spinel along the contacts of lenticular enclaves of leucocratic gabbro within plagioclase-bearing wehrlite (Fig. 2D). The dominant ore texture is finely disseminated, although some semimassive and massive (more than 80 vol.% chromian spinel) types are also present. Most chromian spinel crystals are unaltered and preserve their magmatic composition. Nevertheless, some grains have a well-developed network of fractures, commonly filled by serpentine and chlorite. Where open fractures are occupied by chlorite, the rim of the spinel grains shows a spongy texture with optical properties and chemical compositions distinct from their respective unaltered core. The altered rim shows a higher Fe_2O_3 content than the unaltered core and is referred to as ferrian chromite.

Primary olivine and pyroxenes (Cr-rich diopside and enstatite) occur both as inclusions within chromian spinel and in the intercumulus silicate matrix. Intercumulus silicates are replaced by secondary hydrous silicates of either high-temperature (*i.e.*, edenite) or low-temperature (serpentine or chlorite) origin. A singularity of the Ouen Island chromitites is that, unlike the other occurrences of chromitite in the New Caledonia ophiolite, they do not record any evidence of subaerial weathering (*i.e.*, laterization).

Major and minor elements in magmatic chromian spinel

Chromian spinel from the three chromitite occurrences is systematically poor in Fe_2O_3 (<5 wt.%) (Fig. 3A, Table 1). Its Cr# is similar in occurrence 1 (0.58–0.61) and occurrence 2 (0.57–0.62), but lower in occurrence 3 (0.52–0.55). In contrast, Mg# is higher in the chromian spinel of occurrences 2 and 3 (0.69–0.72, 0.64–0.69 respectively) than that of occurrence 1 (Mg# in the range 0.57–0.61, Fig. 3B, Table 1). All compositions correspond to Fe-rich magnesiochromite.

Gallium, Ni, V and Sc correlate positively with one another and negatively with Cr# (Table 2). Gallium varies from 26 to 31 ppm in chromian spinel of occurrence 1, from 30 to 34 ppm in occurrence 2, and from 42 to 47 ppm in occurrence 3. Nickel increases from 554 to 583 ppm in occurrence 1, to 712–804 ppm in occurrence 2, and to 787–904 ppm in occurrence 3. Vanadium ranges from 1070 to 1163 ppm in chromian spinel of occurrence 1, from 1063 to 1097 ppm in that of occurrence 2, and from 1137 to 1230 ppm in that of occurrence 3. Scandium contents are very low, ranging from 2 to 4 ppm in the three occurrences of chromitite.

The Ti contents in chromian spinel are low (<1341 ppm), and correlate negatively with Mg#, as do the contents of Zn, Co, and Mn (Table 2). Thus, chromian spinel of occurrences 1 and 3 show higher Ti (1323–1341 ppm and 641–687 ppm, respectively) than those of occurrence 2 (508–535 ppm). Chromian spinel of occurrences 1 and 3 is richer in Zn (736–811 ppm and 520–562 ppm, respectively) than that of occurrence 2 (425–452). Cobalt is also higher in the lower-Mg# chromian spinel of occurrences 1 and 3 (302–319 ppm

FIG. 1. Geographical location and schematic geological map of Ouen Island, showing the main geological units and the location of the chromitite occurrences investigated.

and 231–260 ppm, respectively) than in occurrence 2 (186–207 ppm). Manganese is enriched in chromian spinel of occurrences 1 and 3 (1681–1769 ppm and 1255–1417 ppm) relative to that of occurrence 2 (1212–1543 ppm).

Some grains of chromian spinel grains in occurrence 1, showing an identical distribution of the major elements Al Cr and Fe, are, however, distinctly enriched in Mn (2305–2484 ppm), Co (426–479 ppm) and Zn (1086–1438 ppm) (Table 2). High levels of Mn, Co, and Zn have also been reported in altered and re-equilibrated chromian spinel from podiform chromitites in ophiolite complexes (*e.g.*, Pagé & Barnes 2009, Singh & Singh 2011). If these grains are excluded, we can argue that the minor and trace elements in the spinel phase of the Ouen Island chromitites have not been significantly disturbed by alteration, and thus reflect the compositions imposed during the magmatic stage.

The distribution patterns of major, minor and trace elements in the Ouen Island chromitites, normalized to chromian spinel from MORB, are comparable to those reported for chromian spinel from podiform chromitites of the Thetford Mines ophiolite (Pagé & Barnes 2009) (Figs. 3C–E). Chromian spinel from the Ouen Island chromitites shows slight depletion in Al, Ga, Ti and Mg, and slight enrichment in Zn, Co, Mn and Fe, compared with chromian spinel from MORB. Moreover, it also has strong anomalies in V (positive) and Sc (negative) that were not reported by Pagé & Barnes (2009) from the Thetford Mines chromitite (Figs. 3C–E).

TABLE 1. REPRESENTATIVE COMPOSITIONS OF THE UNALTERED CORE OF CHROMIAN SPINEL GRAINS IN CHROMITITES OF OUEN ISLAND

	1	2	3	4	5	6	7	8
SiO_2 wt.%	0.02	0.03	0.10	0.02	0.23	0.04	0.06	0.01
TiO_2	0.34	0.17	0.31	0.12	0.06	0.11	0.07	0.04
V_2O_5	0.21	0.16	0.20	0.23	0.24	0.25	0.29	0.25
Al_2O_3	21.75	22.21	20.37	20.22	22.71	25.44	24.67	23.63
Cr_2O_3	46.55	45.99	47.58	49.29	45.24	42.15	42.78	42.76
FeO	16.44	16.32	15.39	11.39	10.94	12.86	13.52	13.61
Fe_2O_3	1.79	1.86	2.09	2.85	2.95	2.90	3.53	4.39
MnO	0.12	0.14	0.31	0.28	0.15	0.11	0.18	0.15
MgO	12.51	12.34	12.76	15.36	15.60	14.88	14.54	14.18
CoO	0.01	0.04	0.05	0.02	0.00	0.00	0.00	0.01
NiO	0.09	0.01	0.06	0.21	0.12	0.04	0.00	0.00
ZnO	0.00	0.23	0.00	0.00	0.07	0.10	0.00	0.14
Total	99.82	99.51	99.21	99.99	98.29	98.86	99.64	99.15
Cr ppm	1.14	1.13	1.18	1.19	1.10	1.01	1.03	1.04
Ti	0.01	0.00	0.01	0.00	0.00	0.00	0.00	0.00
V	0.00	0.00	0.00	0.00	0.00	0.00	0.00	0.00
Al	0.79	0.81	0.75	0.73	0.82	0.91	0.88	0.85
Fe^{3+}	0.04	0.04	0.05	0.07	0.07	0.07	0.08	0.10
Fe^{2+}	0.43	0.42	0.40	0.29	0.28	0.33	0.34	0.35
Mn	0.00	0.00	0.01	0.01	0.00	0.00	0.00	0.00
Mg	0.58	0.57	0.60	0.70	0.71	0.67	0.66	0.65
Co	0.00	0.00	0.00	0.00	0.00	0.00	0.00	0.00
Ni	0.00	0.00	0.00	0.01	0.00	0.00	0.00	0.00
Zn	0.00	0.01	0.00	0.00	0.00	0.00	0.00	0.00
Cr#	0.59	0.58	0.61	0.62	0.57	0.53	0.54	0.55
Mg#	0.58	0.57	0.60	0.71	0.72	0.67	0.66	0.65
Fe^{3+}#	0.02	0.02	0.03	0.03	0.04	0.03	0.04	0.05

The analyses were made with an electron microprobe. Occurrence 1: 1–3, occurrence 2: 4–5, occurrence 3: 6–8.

PGE Geochemistry and PGM Mineralogy

The Ouen Island chromitites are strongly enriched in Pt and Pd (up to 11.5 ppm Pt + Pd), and the absolute concentrations of PGE vary greatly (Table 3), increasing from chromitites of occurrence 1 (0.1–0.5 ppm) to those of occurrence 2 (1.2–2.6 ppm) and occurrence 3 (1.8–11.5 ppm). The PGM minerals are clearly dominated by minerals of both Pt and Pd (201 grains from a total of 250 PGM grains identified, Table 4), which also are distributed irregularly: 148 PGM grains were discovered in five chromitite samples from occurrence 3, 61 PGM grains in four chromitite samples from occurrence 2, and 60 PGM grains in three samples from occurrence 1.

The PGM occur as small inclusions, usually <20 μm across, in the unaltered core of chromian spinel or in intercumulus with respect to the primary silicates (olivine or pyroxenes). They are also located along fractures cutting across chromian spinel crystals, in secondary silicates of the interstitial silicate matrix (*i.e.*, amphibole, serpentine and chlorite) and in the altered rim of ferrian chromite (Table 4). The PGM found as inclusions in the unaltered core of chromian spinel or in primary silicates tend to be euhedral or less commonly subhedral, whereas PGM in altered zones of the chromitite exhibit irregular shapes with a corroded outline or porous textures.

TABLE 2. COMPOSITION OF CORE OF CHROMIAN SPINEL GRAINS IN THE OUEN ISLAND CHROMITITES

	Occurrence 1				Occurrence 2		Occurrence 3		M.D.L.
	OUE-R06 *n* = 4		OUE-R06* *n* = 6		OUE-R25 *n* = 10		OUE-R50 *n* = 10		
	Min.	Max.	Min.	Max.	Min.	Max.	Min.	Max.	
Sc ppm	2	3	3	4	2	3	3	4	0.05
Ti	1323	1341	1525	1795	508	535	641	687	0.12
V	1070	1163	1500	1785	1063	1097	1137	1230	0.01
Mn	1681	1769	2305	2484	1212	1543	1255	1417	0.18
Co	302	319	426	479	186	207	231	260	0.005
Ni	554	583	732	809	712	804	787	904	0.05
Zn	736	811	1086	1438	425	452	520	562	0.07
Ga	26	31	37	54	30	34	42	47	0.02
Cr#	0.58-0.61				0.62		0.52-0.54		
Mg#	0.57-0.61				0.69-0.71		0.67-0.69		

Minor- and trace-element data on the core were acquired by LA–ICP–MS. An asterisk indicates that the core has been influenced by postmagmatic alteration and re-equilibration. M.D.L.: minimum detection limits at 99% confidence.

PGM and associated BMS in unaltered zones of the chromitite

The PGM assemblage in the unaltered core of chromian spinel grains comprises a Pt–Fe alloy, Pt–(Rh–Pd) sulfides (cooperite and malanite), Ru–Os–Ir sulfides (laurite and an unidentified Ir–S compound), native Ru and Pd and an unidentified Pd–Te mineral (Table 4).

The Pt–Fe alloy is by the far the most abundant PGM encountered in the unaltered core of chromian spinel. It consists chiefly of Pt (82.19–87.15 wt.%) and Fe (9.31–10.65 wt.%), with minor incorporation of Pd (<1.70 wt.%) and Ni + Cu (<3.10 wt.%) (Fig. 4A, Table 5, anal. 1–2). The composition of the Pt–Fe alloy is consistent with an isoferroplatinum-type stoichiometry (Pt_3Fe), although a precise classification is hampered by the lack of reliable X-ray-diffraction data. Hereafter, we will refer to this phase as "Pt–Fe alloy" for convenience. This alloy forms single isolated crystals (Fig. 5A), two-phase grains with pentlandite or laurite (Fig. 5B) and polyphase aggregates with cooperite ± malanite ± Ir–S ± Pd–Te (Fig. 5C).

Cooperite deviates slightly from the ideal stoichiometry, PtS, owing to replacement of Pt by other elements: 4 wt.% Fe, 2.83% Pd, 1.13% Rh, 0.68% Ni (Table 5, anal. 3–4). It is found associated with larger grains of Pt–Fe alloy or surrounded by base-metal sulfides (BMS: heazlewoodite, chalcopyrite and pentlandite) (Fig. 5D).

Malanite also deviates from the ideal composition ($CuPt_2S_4$) owing to replacement of Pt by others PGE (14.62 wt.% Rh, 5.10% Ir, 3.68% Pd), and Cu by Ni and Fe (5.24% Ni+Fe) (Fig. 6A, Table 5, anal. 5–6). No grains of malanite were found as isolated inclusions; it invariably occurs associated with other PGM (Pt–Fe

TABLE 3. WHOLE-ROCK Pt AND Pd CONTENTS IN THE SAMPLES OF THE OUEN ISLAND CHROMITITE INVESTIGATED

Sample	Pt (ppb)	Pd (ppb)	Total (ppm)
Occurrence 1			
OUE-R07	460	23	0.5
OUE-R03	196	23	0.2
OUE-R06	127	17	0.1
Occurrence 2			
OUE-R23	2400	182	2.6
OUE-R25	2330	120	2.5
OUE-R29	1740	220	2
OUE-R26	1120	103	1.2
Occurrence 3			
OUE-R13	1640	126	1.8
OUE-R54	10600	888	11.5
OUE-R80	8830	618	9.4
OUE-R11	5820	424	6.2
OUE-R50	5640	500	6.1

TABLE 4. ABUNDANCES OF THE VARIOUS PGM AND BMM SPECIES IN MICROTEXTURAL SETTINGS WITHIN THE OUEN ISLAND CHROMITITES

	UC	FC	F			M			
			SF	Chl	Srp	PS	Amp	Chl	Srp
PGE alloys									
Pt-Fe alloy	19	2		14	3	2		16*	5
Tulameenite				6				14	
(Pt-Pd-Rh)-BM alloys		1		16				12	
Native PGE									
Os		3		3					1
Ru	3								1
Pt				1					
Pd	1	1							2
Pt-(Rh-Pd) sulfides									
Cooperite	9							1*	
Malanite	3		1	3*	8*		6*		9*
Rh-S						1			
Ru-(Os-Ir) sulfides									
Laurite	9	6	1	5*	5*	3		3*	4*
Os-S (erlichmanite ?)						1			
Ir-S	1								
(Ir-Rh) sulfarsenides									
(Ir-Rh)-As-S (Irs-Hlw?)		3		2					
Pd compounds									
Pd-Te	1								
Pd-Sb				1					
Pd-Hg				1					
Pt oxides									
Pt oxides				30					
Ni-Fe sulfides									
Pentlandite	34	16	4	7*	17*		6*	4*	9*
Heazlewoodite	3				9				
Millerite	4	1			5	1			
Cu-Fe sulfides									
Chalcopyrite	14				1*	1			
Bornite	12	2*				1			
Ni-Fe-Cu alloys									
Awaruite		28			9				9
Native Cu				9				3	
Ni sulfarsenides									
Ni-As-S (gersdorffite ?)								1	

UC: unaltered core of chromian spinel, FC: ferrian chromite rim, F: fracture, M: interstitial matrix. SF: silicate-free, PS: primary silicate, Amp: amphibole, Chl: chlorite, Srp: serpentine. (*) pre-existing altered mineral. Symbols: Irs: irarsite, Hlw; hollingworthite.

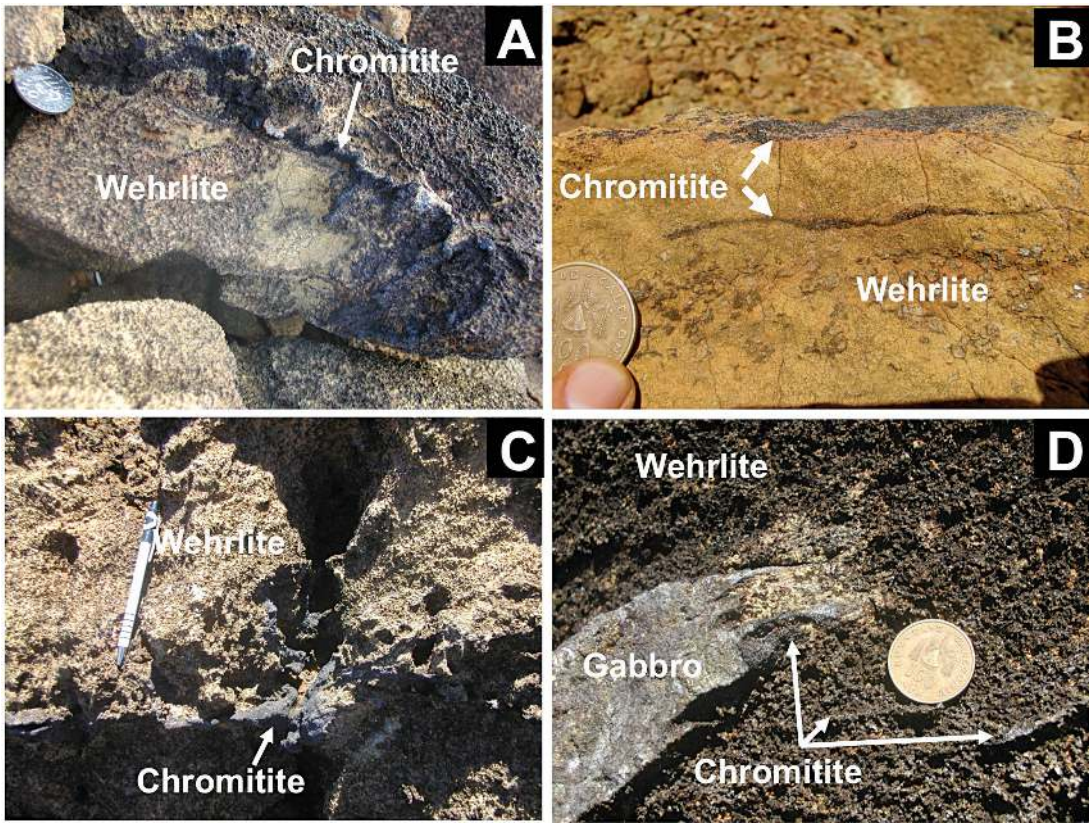

FIG. 2. Field images of the Ouen Island chromitites. (A) Schlieren of chromitite from occurrence 1, hosted in plagioclase-bearing wehrlite. (B) Irregular chromitite of occurrence 2 in plagioclase-bearing wehrlite. (C) Irregular chromitite of occurrence 3. (D) Chromitites at the contact between plagioclase-bearing wehrlite and enclave of anorthositic gabbro in occurrence 3.

alloy ± cooperite ± Ir–S ± Pd–Te) (*e.g.*, Fig. 5C) or pentlandite.

Laurite (ideally RuS_2) shows a very limited Os-for-Ru substitution (Os varies between 0.96 and 15.7 wt.%) (Fig. 6B). This composition is similar to that of laurite from layered complexes (Fig. 6B, Table 5, anal. 7–8). Some of the analyzed grains display zoning characterized by bands with variable Os contents (Figs. 5E, 6B).

The PGM assemblage associated with olivine and pyroxenes in the silicate matrix comprises the Pt–Fe alloy, laurite and two other sulfides only qualitatively identified: a sulfide containing Os and S, very probably erlichmanite, and another containing Rh and S. Most PGM grains hosted in these interstitial silicates have rounded shapes, suggesting their entrapment in a state close to liquid by growing silicates. Nevertheless some polygonal PGM grains oriented along the cleavage of pyroxenes were also observed (*e.g.*, Fig. 5F).

About 69 grains of BMS were found in close association with PGM within unaltered cores of chromian spinel grains and in the interstitial primary silicates (Table 4). They are, in order of abundance: pentlandite, Cu–Fe sulfides (chalcopyrite and bornite) and Ni sulfides (millerite and heazlewoodite) (Table 4). These BMS display size and morphological features similar to those of the PGM. In composite aggregates composed only of BMS, the more Fe-poor sulfides invariably occupy the external parts of the inclusion (*e.g.*, Figs. 5G–H). Some large grains of pentlandite found in the unaltered core of chromian spinel grains contain small blebs (< 1 μm) of Ru or Pd (analyzed only qualitatively) at their margins.

PGM and associated BMM in altered zones of the chromitite

The PGM assemblage in altered zones of chromitite comprises the PGM already described from unaltered grains (Pt–Fe alloy, laurite, malanite, Pd and Ru), tulameenite, complex alloys of Pt–Pd–Rh and base metals

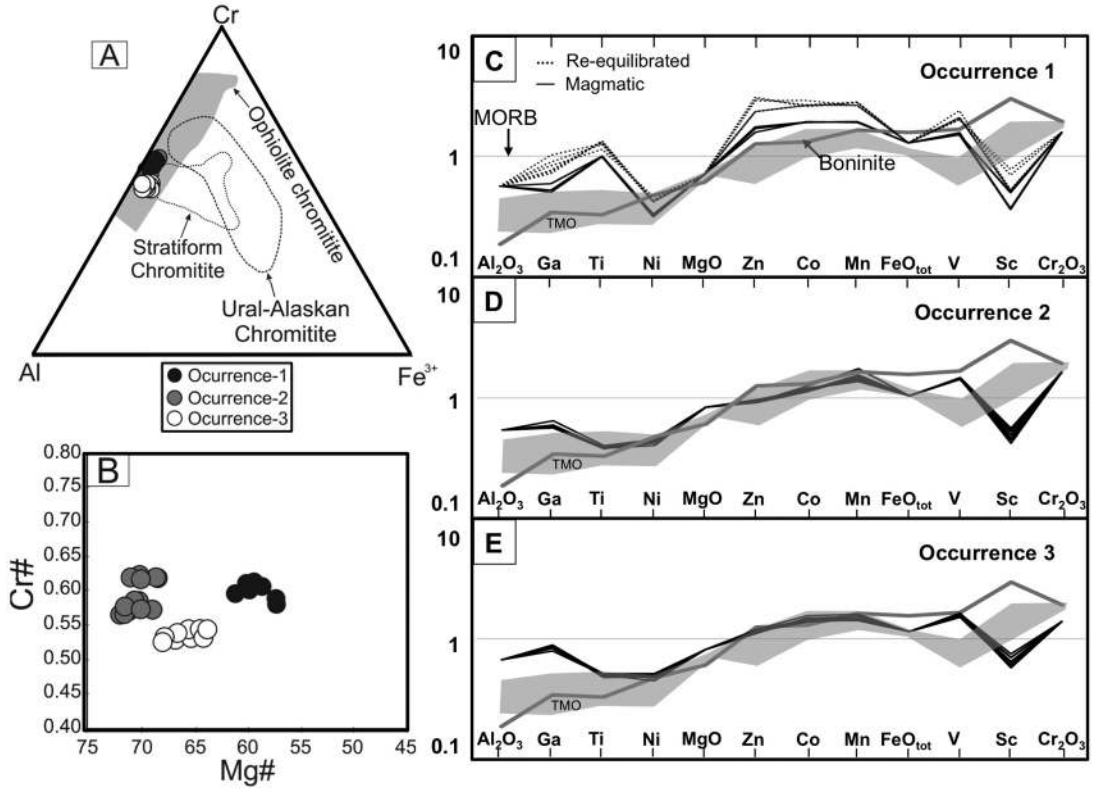

FIG. 3. Compositions of primary chromian spinel of the Ouen Island chromitite, compared with chromian spinel of various tectonic settings (data sources after Proenza *et al.* 2007). (A) Al–Cr–Fe^{3+}. (B) Cr# [Cr/(Cr+Al)] *versus* Mg# [Mg/(Mg+Fe)]. (C–E) spidergrams showing the distribution of major and minor elements in chromian spinel from chromitite occurrences 1 (C), 2 (D) and 3 (E). Data are normalized to chromite from MORB and compared with chromian spinel from boninitic lavas (Pagé & Barnes 2009). TMO: Cr-rich chromian spinel from podiform chromitite of the Thetford Mines ophiolite (Pagé & Barnes 2009).

(BM), native metals (Os and Pt), Pt oxides, undetermined Pd phases with Sb and Hg, sulfarsenides of Ir and Rh, and PGE-bearing pentlandite.

The PGM occurring in unaltered and altered zones exhibit compositional differences, which can be related to morphological features. Thus, grains of Pt–Fe alloy associated with chlorite (showing corroded borders) are richer in Pd (up to 7 wt.% Pd) than those enclosed in unaltered chromian spinel (Fig. 4B, Table 6, anal. 1–6). Some Pt–Fe alloy grains found in fractures associated with chlorite form composite aggregates with unidentified phases consisting of (Ir–Rh)–As–S, probably irarsite–hollingworthite, or with Pd compounds (*i.e.*, Pd–Sb or Pd–Hg). Some Pt–Fe alloy grains associated with chlorite are replaced by tulameenite (Pt in the range 73–75.4 wt.%, Fe in the range 10.04–13.12%, Pd <3.35% and Ni+Cu < 13.25%) (Figs. 4B and 7A, Table 6, anal. 7–8). The presence of tulameenite as a replacement product of Pt–Fe alloy is intimately related to the occurrence of nearby large grains of native Cu (Table 4). Tulameenite grains, particularly those found in the silicate matrix, commonly exhibit a rim of (Pt–Pd–Rh)–BM alloys (*e.g.*, Fig. 7B). Unlike the grains of Pt–Fe alloy associated with chlorite, those associated with serpentine do not show any evidence of alteration. They have a perfectly euhedral shape, generally associated in polyphase aggregates with byproducts from the decomposition of pentlandite (*i.e.*, assemblages consisting of heazlewoodite ± awaruite ± magnetite) (Fig. 7C).

Although a few sulfides phases associated with secondary silicates (*i.e.*, amphibole, chlorite or serpentine) retain their original composition, most show evidence of sulfur loss (desulfurization). Thus, the alteration of laurite involves remobilization of Os, which is then deposited along grain boundaries as native Os (Fig. 7D). In contrast, desulfurization of malanite involves a decrease of volume, which is counterbal-

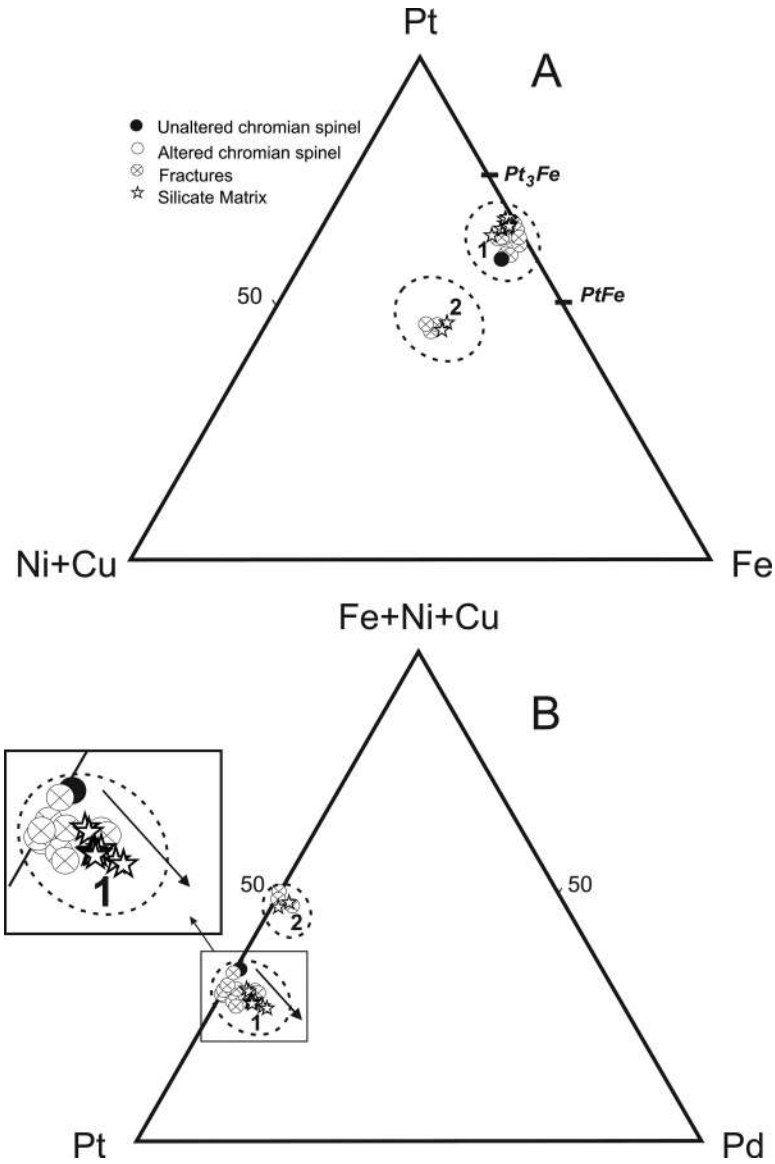

FIG. 4. Compositions of the PGM. (A) Pt-dominated alloys from chromitites of Ouen Island, in the Pt (+Pd) – Fe – Ni + Cu plot and (B) the Fe + Ni + Cu – Pd – Pt diagram. Arrow in the extended window shows the almost continuous trend of increasing of Pd from grains of Pt–Fe alloy within unaltered chromian spinel toward those in altered zones of the chromitite (*i.e.,* fractures, silicate matrix). Field 1: Pt–Fe alloys, field 2: tulameenite.

anced by the introduction of base metals, mainly Cu, without remobilization of the PGE (Figs. 6A, 7E, Table 7, anal. 1–4). Pentlandite enriched in PGE, occurring in fractures free of silicates or within amphibole, is associated with malanite or laurite (Fig. 7F). This pentlandite is rich in Ni (Ni/Fe in the range 0.48–20.02) and contains up to 2.20 wt.% Ru, and 8.58% Rh in ruthenian and rhodian pentlandite, respectively (Table 7, anal. 5–8).

Platinum oxides show a beige or brownish color, appreciable pleochroism and strong anisotropy under reflected light. Their reflectivity is much lower than

that of the other PGM. The Pt oxides occur as single grains on partially desulfurized malanite (Fig. 7G) or, more commonly, as isolated grains (Fig. 7H). They show a characteristically granular internal texture, with a rugged aspect, and in some cases, radial fractures, a sign of volume loss (Fig. 5H). These features are similar to those reported for other Pt oxides described in New Caledonia and in the literature (*e.g.*, Augé & Legendre 1994, Locmelis *et al.* 2010). Like PGE-rich oxides reported in the literature, the Pt oxides of the Ouen Island chromitites give low analytical totals (<85 wt.%) (Table 8, anal. 1–8). These results, here considered as being semiquantitative, show a predominance of Pt over base metals (Ni, Fe and Cu), and traces of other PGE and S. Such compositions define a single group (Fe + Ni + Cu) – S – (Pt + Ir + Rh) in a triangular plot (Fig. 6A), clearly different from their probable precursor, malanite. We also find that Pt oxides in the silicate matrix, which probably were more strongly affected by alteration-inducing fluids, are residually enriched in PGE (Fig. 6A).

TABLE 5. REPRESENTATIVE COMPOSITIONS OF PGM GRAINS LOCATED IN THE UNALTERED CORE OF CHROMIAN SPINEL GRAINS

	1	2	3	4	5	6	7	8
Os wt.%	0.0	0.2	0.0	0.0	0.0	0.0	13.0	8.2
Ir	2.1	1.0	0.1	0.0	4.9	4.9	0.8	1.2
Ru	0.2	0.0	0.0	0.0	0.0	0.0	47.7	51.8
Pt	82.7	83.8	78.2	78.7	33.1	33.3	0.1	0.0
Pd	1.7	0.9	2.8	2.7	3.3	3.6	0.1	0.2
Rh	2.4	0.3	1.1	1.1	14.1	13.4	0.9	1.0
Fe	9.8	10.1	4.0	3.9	1.5	1.6	0.5	0.6
Ni	1.5	1.5	0.7	0.6	4.6	4.5	0.0	0.0
Cu	0.5	0.1	1.1	1.1	10.6	10.4	0.0	0.0
Co	0.0	0.1	0.0	0.0	2.1	2.7	0.0	0.0
S	0.0	0.0	11.0	10.8	23.8	23.6	34.8	35.0
As	0.0	0.0	0.0	0.0	0.0	0.0	0.2	0.0
Sb	0.0	0.0	0.0	0.0	0.0	0.0	0.0	0.0
Te	0.0	0.0	0.1	0.0	0.0	0.0	0.0	0.0
Total	101.00	98.00	99.00	99.01	98.05	98.04	98.06	98.12
Os at.%	0.00	0.18	0.00	0.00	0.00	0.00	4.16	2.57
Ir	1.62	0.80	0.05	0.00	1.81	1.81	0.25	0.37
Ru	0.29	0.00	0.00	0.00	0.01	0.00	28.58	30.60
Pt	61.84	65.36	45.45	46.08	12.01	12.09	0.04	0.00
Pd	2.30	1.24	2.99	2.91	2.22	2.37	0.03	0.13
Rh	3.45	0.39	1.21	1.25	9.70	9.25	0.53	0.61
Fe	25.63	27.55	8.08	7.92	1.93	1.99	0.55	0.65
Ni	3.63	3.93	1.30	1.26	5.51	5.48	0.01	0.00
Cu	1.24	0.31	1.89	2.00	11.75	11.54	0.00	0.00
Co	0.00	0.18	0.00	0.00	2.50	3.26	0.03	0.02
S	0.00	0.00	38.95	38.59	52.54	52.19	65.67	65.05
As	0.00	0.00	0.00	0.00	0.00	0.00	0.15	0.00
Sb	0.00	0.00	0.00	0.00	0.00	0.00	0.00	0.01
Te	0.00	0.05	0.07	0.00	0.00	0.02	0.00	0.00

The analyses were made with an electron microprobe. Columns: 1–2: Pt–Fe alloy; 3–4: cooperite; 5–6: malanite; 7–8: laurite.

TABLE 6. REPRESENTATIVE COMPOSITIONS OF PGM ALLOYS IN ALTERED ZONES OF THE OUEN ISLAND CHROMITITES

	1	2	3*	4*	5*	6*	7	8
Os wt.%	0.00	0.00	0.00	0.00	0.00	0.01	0.00	0.00
Ir	0.00	0.00	0.00	0.00	0.00	0.00	0.00	0.00
Ru	0.00	0.16	0.00	0.00	0.05	0.04	0.05	0.00
Pt	84.48	84.92	82.85	82.45	80.91	80.32	71.54	72.84
Pd	3.08	2.62	4.70	4.91	6.41	7.23	3.12	3.33
Rh	0.10	0.48	0.37	0.43	0.23	0.31	0.45	0.25
Fe	9.16	9.33	9.42	9.47	9.08	9.02	9.84	10.23
Ni	0.58	0.50	1.19	0.97	0.29	0.33	4.69	5.59
Cu	0.63	0.55	1.29	1.22	0.87	0.85	8.29	6.71
Co	0.02	0.02	0.03	0.01	0.03	0.00	0.03	0.07
S	0.00	0.00	0.00	0.00	0.00	0.00	0.00	0.00
As	0.05	0.16	0.10	0.00	0.12	0.00	0.00	0.00
Sb	0.00	0.00	0.00	0.00	0.00	0.00	0.00	0.00
Te	0.00	0.00	0.00	0.00	0.00	0.00	0.00	0.00
Total	98.10	98.74	99.95	99.46	98.00	98.11	98.02	99.01
Os at.%	0.00	0.00	0.00	0.00	0.00	0.01	0.00	0.00
Ir	0.00	0.00	0.00	0.00	0.00	0.00	0.00	0.00
Ru	0.00	0.24	0.00	0.00	0.08	0.06	0.06	0.00
Pt	66.85	66.68	62.13	62.30	62.73	62.04	46.54	47.14
Pd	4.47	3.77	6.46	6.80	9.11	10.24	3.72	3.94
Rh	0.15	0.71	0.53	0.62	0.34	0.45	0.56	0.31
Fe	25.32	25.59	24.68	24.99	24.58	24.34	22.36	23.12
Ni	1.53	1.30	2.97	2.44	0.76	0.85	10.15	12.01
Cu	1.53	1.33	2.97	2.83	2.08	2.02	16.56	13.33
Co	0.05	0.05	0.07	0.03	0.08	0.00	0.06	0.15
S	0.00	0.00	0.00	0.00	0.00	0.00	0.00	0.00
As	0.10	0.33	0.20	0.00	0.25	0.00	0.00	0.00
Sb	0.00	0.00	0.00	0.00	0.00	0.00	0.00	0.00
Te	0.00	0.00	0.00	0.00	0.00	0.00	0.00	0.00

The analyses were made with an electron microprobe. All analyzed grains are associated with chlorite. Columns: 1–4: Pt–Fe alloy in fractures; 5–6: Pt–Fe alloys in the interstitial matrix; 7–8: tulameenite in fractures.
*: Corroded grain.

Discussion and Conclusions

Origin of the enrichment in Pt and Pd

The Ouen Island chromitites, unlike the IPGE-rich podiform chromitites hosted by the mantle section of the New Caledonia ophiolite (Massif du Sud), are strongly enriched in Pt + Pd. Such enrichment, and the presence of Pt–Fe alloys, resemble the situation in the banded chromitites of the crustal sequence of this ophiolite (Pirogues mineralization, Augé & Maurizot 1995). However, unlike the latter, the Ouen Island chromitites are characterized by a high abundance of sulfides. The formation of the Ouen Island chromitites thus required a parental melt or fluid much more enriched in Pt + Pd than that from which the mantle chromitites crystallized, but in turn with much higher S values than those responsible for the formation of the crustal chromitites.

In terms of major elements, Cr# and Mg#, the composition of the chromian spinel from the Ouen Island chromitites matches well the composition of chromian spinel equilibrated with MORB melts (Arai 1992, Barnes & Roeder 2001), suggesting that these could form from melts of tholeiitic affinity. However,

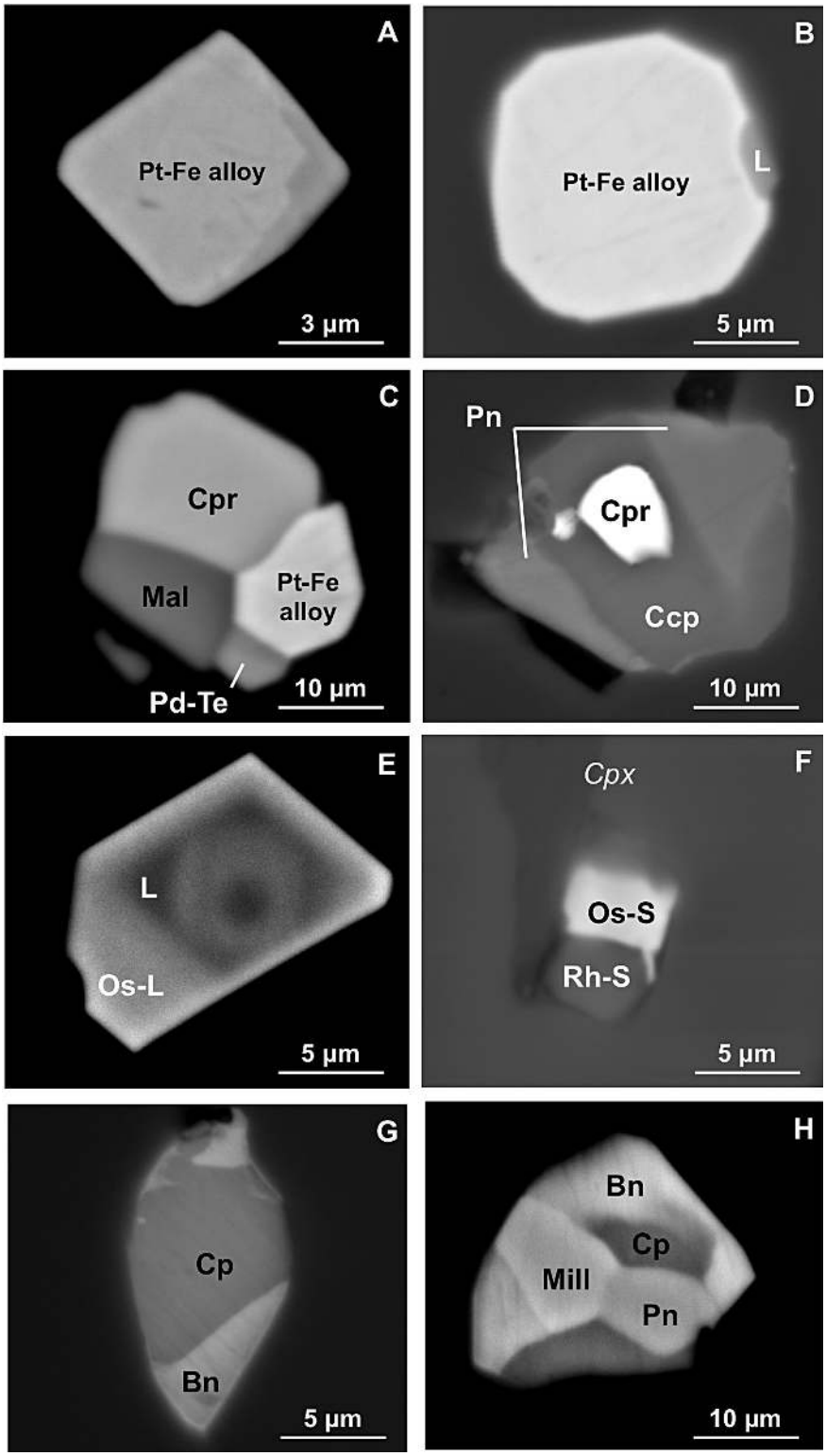
A
Pt-Fe alloy
3 μm
B
Pt-Fe alloy
L
5 μm
C
Cpr
Mal
Pt-Fe alloy
Pd-Te
10 μm
D
Pn
Cpr
Ccp
10 μm
E
L
Os-L
5 μm
F
Cpx
Os-S
Rh-S
5 μm
G
Cp
Bn
5 μm
H
Bn
Cp
Mill
Pn
10 μm

most MORB-like tholeiitic melts generated in ophiolite settings are impoverished in PGE (*e.g.*, Prichard *et al.* 2008, and references therein). On the other hand, chromian spinel from the Ouen Island chromitite is depleted in Ti, Ni and Sc, slightly depleted in Al, Ga, Mg, and enriched in Mn, V, Cr and slightly enriched in Zn, Co and Fe with respect to MORB spinels (Figs. 3C–E). This chromian spinel from the Ouen Island chromitites thus would have crystallized from a melt different from MORB. If we exclude Al, Ga and Sc, the distribution patterns of chromian spinel from the chromitites studied roughly coincides with that of spinel from podiform chromitites produced by melts of boninitic affinity. These types of arc melts, which are believed to have formed by remelting of previously depleted peridotites, are well known to be significantly enriched in PGE (González-Jiménez *et al.* 2011, and references therein).

It has been shown by empirical (Pagé & Barnes 2009, Dare *et al.* 2009) and experimental studies (Mallmann & O'Neill 2009) that Al, Ga, V and Sc contents correlate positively with $f(O_2)$ in chromian spinel. This leads us to suggest that the selective enrichment of incompatible elements shown by chromian spinel of the Ouen Island chromitites was associated with a high $f(O_2)$ in the parental melt(s). This situation is typical in the forearc mantle wedge of suprasubduction zones, where relatively oxidized melts can form (Parkinson & Arculus 1999).

Marchesi *et al.* (2009) showed that wehrlite of the MTZ at Montagne de Sources (Massif du Sud), equivalent to that hosting the Ouen Island chromitites, formed as result of the reaction between pre-existing dunite and

TABLE 7. REPRESENTATIVE COMPOSITIONS OF PGM SULFIDES IN ALTERED ZONES OF THE OUEN ISLAND CHROMITITES

	1*	2*	3*	4*	5	6	7	8
Os wt.%	0.00	0.00	0.00	0.00	0.00	0.00	0.00	0.40
Ir	0.00	0.00	0.00	0.00	0.00	0.12	0.00	0.00
Ru	0.00	0.00	0.00	0.02	2.64	1.64	2.05	2.08
Pt	33.59	33.59	48.60	41.63	0.00	0.00	0.19	0.02
Pd	0.56	1.68	1.55	1.88	0.21	0.00	0.00	0.00
Rh	0.16	0.10	0.29	0.42	7.75	7.95	0.67	0.82
Fe	5.18	5.29	5.59	3.42	24.88	25.23	27.89	27.99
Ni	6.44	9.18	10.62	10.46	29.11	29.36	34.95	34.52
Cu	43.96	38.92	18.34	28.36	0.06	0.00	0.13	0.17
Co	0.07	0.10	0.10	0.00	1.54	1.61	0.76	0.73
S	6.12	7.32	9.24	9.28	31.02	31.03	32.74	32.59
As	0.23	0.22	0.00	0.00	0.00	0.00	0.12	0.02
Sb	0.00	0.00	0.01	0.00	0.00	0.00	0.00	0.00
Te	0.04	0.00	0.20	0.22	0.01	0.03	0.01	0.00
Total	96.35	96.40	94.54	95.70	97.22	96.98	99.52	99.34
Os at.%	0.00	0.00	0.00	0.00	0.00	0.00	0.00	0.10
Ir	0.00	0.00	0.00	0.00	0.00	0.03	0.00	0.00
Ru	0.00	0.00	0.00	0.02	1.28	0.80	0.94	0.96
Pt	13.57	13.40	22.10	17.61	0.00	0.00	0.05	0.00
Pd	0.42	1.23	1.29	1.46	0.10	0.00	0.00	0.00
Rh	0.12	0.08	0.25	0.34	3.69	3.79	0.30	0.37
Fe	7.32	7.37	8.87	5.06	21.84	22.13	23.12	23.30
Ni	8.64	12.16	16.05	14.70	24.32	24.50	27.56	27.33
Cu	54.53	47.65	25.59	36.81	0.05	0.00	0.09	0.12
Co	0.09	0.13	0.15	0.00	1.28	1.34	0.60	0.58
S	15.03	17.76	25.55	23.87	47.43	47.40	47.26	47.23
As	0.24	0.23	0.00	0.00	0.00	0.00	0.07	0.01
Sb	0.00	0.00	0.01	0.00	0.00	0.00	0.00	0.00
Te	0.02	0.00	0.14	0.14	0.00	0.01	0.00	0.00

The analyses were made with an electron microprobe. Samples: 1: desulfurized malanite in silicate-free fracture; 2: desulfurized malanite in fracture filled by serpentine; 3–4: desulfurized malanite associated with amphibole of the interstitial matrix; 5–6: rhodian pentlandite in silicate-free fracture; 7-8: ruthenian pentlandite in silicate-free fracture. *: Corroded grain.

FIG. 5. Back-scattered electron images of representative PGM and BMS in unaltered zones of the Ouen Island chromitites. A–E and G–H: inclusions in core of unaltered chromian spinel. F: inclusions in an unaltered pyroxene crystal of the interstitial silicate matrix. Note that the grains occur oriented along with cleavage of the pyroxene (marked by the darker zone). Key for PGM: Cpr: cooperite, Mal: malanite, Pd–Te: undetermined Pd–Te compound, L: laurite, Os–L: Os-rich laurite, Os–S: undetermined Os–S sulfide (probably erlichmanite), Rh–S: undetermined Rh–S sulfide. Key for BMS: Pn: pentlandite, Ccp: chalcopyrite, Bn: bornite, Mill: millerite. Key for host minerals: Chr: chromite, Cpx: clinopyroxene.

TABLE 8. REPRESENTATIVE COMPOSITIONS OF Pt OXIDES FOUND IN ALTERED ZONES OF THE OUEN ISLAND CHROMITITES

	1	2	3	4	5	6	7	8
Os wt.%	0.00	0.00	0.07	0.00	0.00	0.00	0.00	0.00
Ir	0.30	0.23	0.00	0.00	0.00	0.00	0.00	0.22
Ru	0.00	0.03	0.00	0.00	0.00	0.00	0.06	0.00
Pt	50.98	58.08	47.03	51.66	50.01	65.70	58.72	64.21
Pd	0.79	0.08	6.40	4.76	7.63	3.73	0.43	5.75
Rh	0.32	0.29	0.18	0.07	0.06	0.35	0.22	0.64
Fe	20.05	9.30	8.99	7.92	8.08	4.01	8.45	1.69
Ni	3.84	6.54	12.42	9.51	10.29	1.47	6.40	1.11
Cu	2.58	6.99	7.34	8.89	7.05	3.01	2.92	3.39
Co	0.07	0.03	0.04	0.04	0.05	0.05	0.37	0.07
S	0.01	0.02	0.12	0.95	0.00	0.18	0.80	0.13
As	0.09	0.00	0.00	0.00	0.00	0.00	0.00	0.00
Sb	0.00	0.00	0.00	0.00	0.00	0.00	0.05	0.00
Te	0.00	0.04	0.00	0.07	0.00	0.00	0.04	0.14
Total	79.03	81.63	82.59	83.87	83.17	78.50	78.46	77.35
Os at.%	0.00	0.00	0.05	0.00	0.00	0.00	0.00	0.00
Ir	0.21	0.17	0.00	0.00	0.00	0.00	0.00	0.23
Ru	0.00	0.04	0.00	0.00	0.00	0.00	0.09	0.00
Pt	35.26	43.02	30.29	33.74	33.71	64.04	46.60	65.91
Pd	1.00	0.11	7.56	5.70	9.43	6.66	0.63	10.82
Rh	0.42	0.41	0.22	0.09	0.08	0.65	0.33	1.25
Fe	48.44	24.06	20.23	18.07	19.03	13.65	23.42	6.06
Ni	8.83	16.10	26.59	20.64	23.05	4.76	16.88	3.79
Cu	5.48	15.89	14.51	17.83	14.59	9.01	7.11	10.68
Co	0.16	0.07	0.09	0.09	0.11	0.16	0.97	0.24
S	0.04	0.08	0.47	3.77	0.00	1.07	3.86	0.81
As	0.16	0.00	0.00	0.00	0.00	0.00	0.00	0.00
Sb	0.00	0.00	0.00	0.00	0.00	0.00	0.06	0.00
Te	0.00	0.05	0.00	0.07	0.00	0.00	0.05	0.22

These compositions result from semiquantitative analyses made with an electron microprobe. All analyzed grains were found in association with chlorite. Columns: 1-7: grains in fractures, 8: grain in the interstitial matrix.

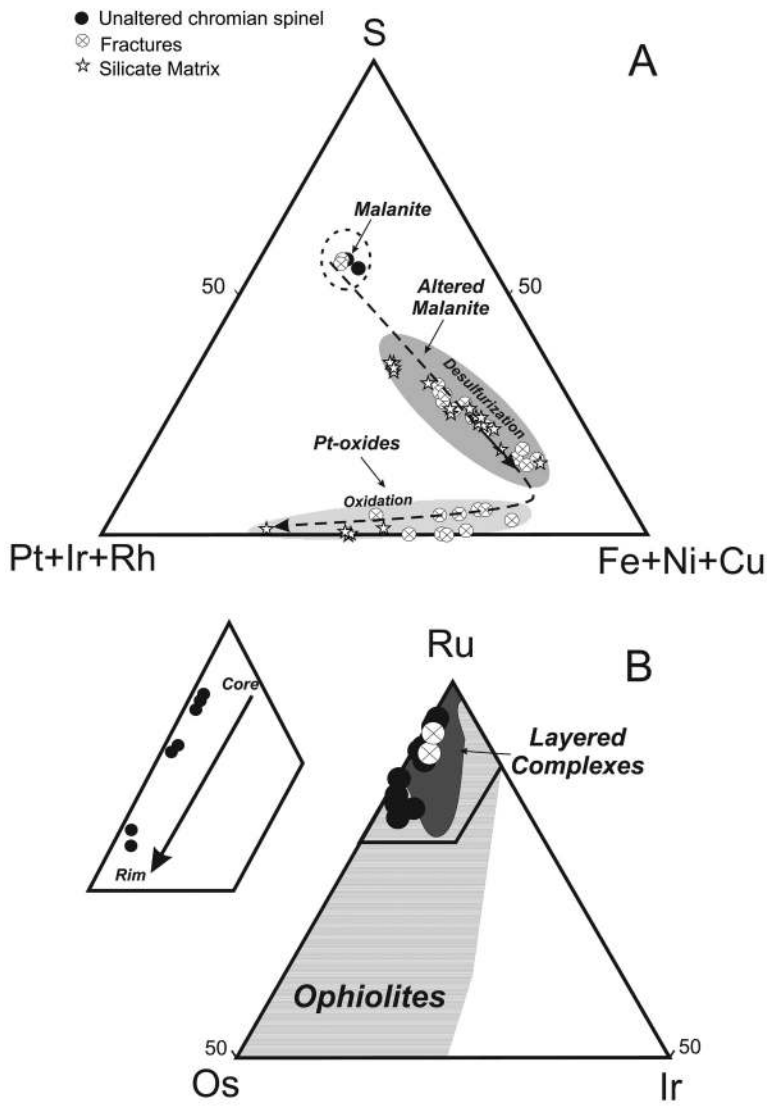

FIG. 6. (A) Composition (at.%) of malanite and PGM oxides in terms of the S – (Fe + Ni + Cu) –(Pt + Ir + Rh). Fields represent the composition of the various mineral species. Dashed arrows indicate the observed alteration trends: desulfurization and oxidation. (B) Chemical composition of laurite from Ouen Island (50 at.%). Fields of laurite inclusions in stratiform chromitite from layered intrusions and mantle-hosted chromitites from various ophiolite complexes are shown for comparison. Compositional variation from core to rim of the zoned laurite included in unaltered chromian spinel is marked by the arrow. Data for stratiform chromitites after Garuti *et al*. (2007).

batches of low-Ti silica-rich melts of boninitic affinity that originated in a forearc suprasubduction zone. Because olivine dissolution and pyroxene-forming reactions proceed with decreasing temperature and melt mass (Kelemen 1990, Kelemen *et al*. 1992, 1995), the formation of wehrlite would drastically reduce the volume of the percolating melts. It can therefore be expected that after extensive melt–rock reaction and fractionation, the residual melts generated in this process became strongly enriched in volatile compo-

nents (McKenzie 1989), constituting small volumes of hydrous silicate melts, from which the Ouen Island chromitites precipitated. These small melt-fractions would also concentrate S, Pt and Pd, as well as Al, Ga, V and Sc, which behave moderately incompatibly during olivine dissolution and the clinopyroxene-forming reactions. These reactions also predict a moderately incompatible behavior of Ni, as the amount of this element released during olivine dissolution is probably not accounted for by the amounts concentrated in the crystallizing clinopyroxene. Evidence for the more effective concentration of the PGE, S and other incompatible elements (Al, Ga, V, Sc) is provided by the fact that the contents of all these elements increase from occurrence 1 to ocurrences 2 and 3. Thus, the chromitites of occurrence 3, which are located in a zone rich in gabbro (supposedly closest to the top of the MTZ sequence) are the richest in PGE and have chromian spinel with the lowest Cr#, and the highest contents of Ga, V, Sc and Ni (Tables 2, 3).

Crystallization of magmatic PGM and BMS assemblages

The predominantly euhedral morphology of PGM and BMS inclusions in the unaltered core of chromian spinel suggests that they crystallized from a magma and were entrapped by growing grains of chromian spinel (*e.g.*, Stockman & Hlava 1984, Augé 1988, Melcher *et al.* 1997, Garuti *et al.* 1999, Gervilla *et al.* 2005, Prichard *et al.* 2008, González-Jiménez *et al.* 2009a). The mineral assemblages and morphological features of the PGM and BMM in the interstitial primary silicates also suggest a magmatic origin, but in this case related to the intercumulus deposition of these phases at the late magmatic stage (*e.g.*, Prichard & Lord 1994, Moreno *et al.* 1999, Prichard *et al.* 2008).

The assemblage made up of Pt–Fe alloy with Os-poor laurite (*e.g.*, Fig. 5A) is stable under sulfide-undersaturated conditions and at temperatures as high as 1100°C (Stockman & Hlava 1984, Roeder & Jamieson 1992, Barin 1995, Brenan & Andrews 2001, Andrews & Brenan 2002, Bockrath *et al.* 2004). In contrast, the formation of assemblages of Pt-rich alloys and Pt ± Pd ± Rh ± Ir sulfides (*e.g.*, Fig. 5C) may take place, as experimentally demonstrated Makovicky & Karup-Møller (2000) and Majzlan *et al.* (2002), at higher $f(S_2)$ and lower temperatures (1100–1000°C) or both. These observations suggest that the PGM have crystallized under increasing sulfur fugacity with decreasing T (*e.g.*, Augé & Johan 1988, Garuti *et al.* 1999). However, the oscillatory zoning shown by some laurite crystals included in unaltered grains of chromian spinel lead us to suggest that the PGM probably formed with a system dominated by short-term variations of $f(S_2)$ and T, rather than from a single fractional crystallization process, followed by settling in a closed magmatic chamber (González-Jiménez *et al.* 2009a). An open-system environment with variations in the physicochemical properties of the parental melt would be a natural consequence of the proposed model of chromitite formation.

According to the proposed model, it should be expected that at the late stages of magmatic evolution, the small-volume hydrous silicate melts would become oversaturated in H_2O, leading to unmixing of a silicate fraction and a H_2O-rich, volatile fraction (Matveev & Ballhaus 2002). In such a scenario, chromian spinel grains (already precipitated) and some small particles of Pt–Fe alloys attached to their surfaces (Ballhaus *et al.* 2006, Prichard *et al.* 2008) would concentrate in the H_2O-rich volatile phase (Matveev & Ballhaus 2002). This unmixing of a silicate melt and a H_2O-rich fraction could also enhance the segregation of sulfide melt(s) (Ballhaus & Stumpfl 1986, Ferrario & Garuti 1990, Melcher *et al.* 1997). Because sulfide melts wet the surfaces of oxides better than silicate liquids, the immiscible sulfide melt(s) would tend to concentrate with a dense phase like chromian spinel in the spinel-laden H_2O-rich pools (Barnes in Augé *et al.* 2005, Holzheid *et al.* 2010). Immiscible segregation of sulfide melt(s) would also produce a further concentration of the available PGE (Makovicky *et al.* 1986, Ballhaus *et al.* 2001, Lorand *et al.* 2010), giving rise to the assemblages containing Pt- and BM-rich sulfides (*e.g.*, PGE-rich pentlandite, malanite and BMS; Figs. 5D, C, H), which now are found within unaltered chromian spinel grains or in primary silicates of the intercumulus matrix. Thus, the combined effect of physical fractionation and the segregation of an immiscible sulfide melt explains the well coexistence of Pt–Fe alloys and sulfides in the primary assemblage, which would have formed within a wide window of $f(S_2)$ and T, as we observe in the Ouen Island chromitites.

The relatively evolved nature of the melts involved in the formation of chromitites, as expected to be found in the uppermost part of the ophiolite section, would also explain the formation of PGM of Te, As, Hg or Sb coeval with alloys and sulfides (*e.g.*, Fig. 5C) (Prichard *et al.* 2008). Nevertheless, the close association of the PGE-bearing compounds of As, Hg or Sb with chlorite in the interstitial altered silicate matrix suggests a secondary, rather than primary origin, as discussed below.

Secondary alteration and neoformation of PGM and BMS

Most sulfides in contact with secondary silicates in altered zones show irregular shapes, as well as evidence for loss of S or remobilization of the PGE. The sulfides, after their deposition, thus may have reacted with fluids with very low $f(S_2)$ and $f(O_2)$ (*e.g.*, Eckstrand 1975, Klein & Bach 2009). The appearance of altered sulfides associated with amphibole replacing olivine

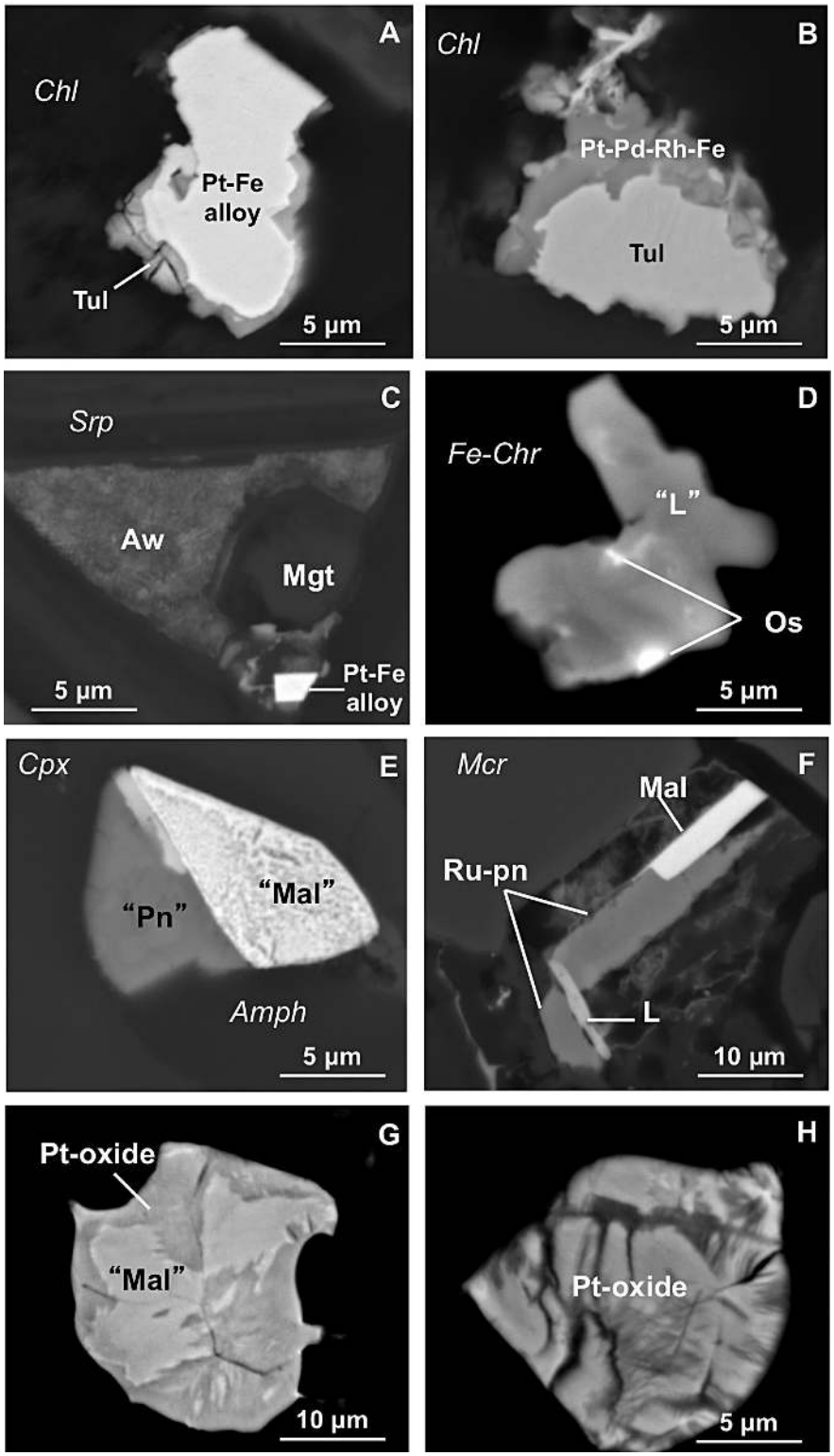
A
Chl
Pt-Fe
alloy
Tul
5 μm
B
Chl
Pt-Pd-Rh-Fe
Tul
5 μm
C
Srp
Aw
Mgt
Pt-Fe
alloy
5 μm
D
Fe-Chr
"L"
Os
5 μm
E
Cpx
"Pn"
"Mal"
Amph
5 μm
F
Mcr
Mal
Ru-pn
L
10 μm
G
Pt-oxide
"Mal"
10 μm
H
Pt-oxide
5 μm

or pyroxene (*e.g.*, Fig. 7E) suggests that an excess of H_2O was present after crystallization of the chromian spinel, leading to the formation of residual high-T hydrothermal fluid. The consumption of S, originally present in the hydrous silicate melt as H_2S, to form sulfides during the late magmatic stages (*e.g.*, Ballhaus & Stumpfl 1986, Ferrario & Garuti 1990, Melcher *et al.* 1997), would lead to the residual concentration of H_2 in the high-T hydrothermal fluid. In such a setting, the reaction of pre-existing sulfides with the reducing fluid(s) would have produced desulfurization of the sulfides, as observed here. On the other hand, the association of partially desulfurized sulfides with low-temperature silicates may be related to their alteration after reaction with reducing fluids generated during the initial stages of serpentinization (*e.g.*, Alt & Shanks 1998, Klein & Bach 2009).

Grains of Pt–Fe alloy associated with amphibole or serpentine in the interstitial matrix, unlike most sulfides, show perfectly euhedral shapes and unmodified chemical compositions (Fig. 7C). These features suggest that the grains of Pt–Fe alloy were not affected by postmagmatic fluids. Furthermore, the common association of these Pt–Fe alloy grains with S-poor sulfides of Ni ± awaruite ± magnetite in microdomains of serpentine in the interstitial matrix suggests that the Pt–Fe alloy remained stable under the reducing environment imposed by the transformation of olivine to serpentine. In contrast, the corroded outlines of Pt–Fe alloy grains associated with chlorite or ferrian chromite suggest that this alloy became unstable when relatively oxidizing fluids, related to the formation of chlorite and ferrian chromite, were present (González-Jiménez *et al.* 2009b). The higher Pd contents of altered Pt–Fe alloy grains associated with chlorite suggest that relatively more oxidized fluids could mobilize Pt from the alloy, leaving residual Pd (Fig. 4B). The remobilization and later redeposition of Pd by these fluids are also suggested by the formation of Pd-rich compounds of Hg or Sb. Other lines of evidence that the PGE, together with base metals and anions, were carried by circulating fluids, are the alteration of the Pt–Fe alloy to tulameenite, the replacement of the latter alloy by (Pt–Pd–Rh)–BM alloys, and the presence of As-rich minerals [*i.e.*, (Ir–Rh)–As–S and gersdorffite], which occur only in association with chlorite and ferrian chromite. The remobilization and redeposition of PGE and base metals by relatively oxidized hydrothermal solutions have been widely documented in chromitites affected by serpentinization and metamorphism (*e.g.*, Thalhammer *et al.* 1990, Yang & Seccombe 1993, Malitch *et al.* 2003, Proenza *et al.* 2008, El Ghorfi *et al.* 2008).

Oxides and hydroxides of PGE have been reported from numerous instances of ophiolite-related chromitites worldwide (*e.g.*, Augé & Legendre 1994, Garuti & Zaccarini 1997, Krstic & Tarkian 1997, Garuti *et al.* 1997, Tsoupas & Economou-Eliopoulos 2008, Zaccarini *et al.* 2009, Uysal *et al.* 2009). The origin of these phases is still a matter of debate; it is uncertain whether the oxygen is bound in oxide or hydroxide form (*e.g.*, Uysal *et al.* 2009, Hattori *et al.* 2010, Locmelis *et al.* 2010). Nevertheless, all these minerals share a set of distinctive characteristics that allow their differentiation from other PGM, such as internal heterogeneity, porosity, low reflectivity and low analytical totals. Genetic models suggest that such PGE oxides may either precipitate directly from hydrothermal fluids or form *in situ* by alteration of a PGM precursor during hydrothermal activity (*e.g.*, Garuti *et al.* 1997) or supergene processes (weathering: Augé & Legendre 1994, Suarez *et al.* 2010, Locmelis *et al.* 2010). In the Ouen Island chromitites, most Pt oxides occur as a rim on partially desulfurized malanite (Fig. 7G). Such textures indicate that the oxides may be derived from *in situ* oxidation of desulfurized sulfides, rather than by direct precipitation from hydrothermal solutions. The lack of evidence for laterization in the Ouen Island chromitites, and the exclusive association of the Pt oxides assemblages with chlorite (Table 4), suggest that the origin of these PGM is related to serpentinization under hydrothermal conditions, as was reported in chromitites of the Nurali massif in the Urals (*e.g.*, Garuti *et al.* 1997) and Muğla in Turkey (Uysal *et al.* 2009). This interpretation, and the present lack of laterization, rule out an origin for the Pt oxides of Ouen Island by laterization, as has been proposed for Pt oxides associated with other chromitites of the New Caledonia ophiolite (*e.g.*, Augé & Legendre 1994).

In summary, we propose that after chromite crystallization from small-volume hydrous silicate melts, the excess of H_2O led to a high-T hydrothermal event, which was followed by and overprinted by a low-T hydrothermal event. However, despite this microtextural study of the distribution of PGM and BMM, we cannot confirm the interaction (and possible mixture) of both types of hydrothermal solutions.

FIG. 7. Back-scattered electron images of representative PGM and BMM in altered zones of the Ouen Island chromitites. A–C: assemblages of Pt-bearing alloys, D–E: assemblages of Pt- and Ru-bearing sulfides. A–C and E: minerals located in the interstitial silicate matrix, D: minerals in altered chromian spinel, F–H: minerals found in open fractures in chromite, filled by chlorite. Key for PGM: Tul: tulameenite, "L": partly desulfurized laurite, Os: native osmium, Mal: malanite, "Mal": partly desulfurized malanite, Ru-pn: ruthenian pentlandite. Key for BMS: "Pn": partly desulfurized pentlandite, Aw: awaruite. Key for host minerals: Chl: chlorite, Srp: serpentine, Fe-Chr: ferrian chromite, Cpx: clynopyroxene, Amph: amphibole.

Acknowledgements

The authors are grateful to C. Gilles (Analysis and Mineral Characterization Laboratory of BRGM, Orléans, France), I. Sánchez Almazo (Centro Andaluz de Medio Ambiente of the Junta Andalucía, University of Granada for their assistance with EPMA and ESEM. We also acknowledge Federica Zaccarini and Evgeny V. Pushkarev for their critical comments on the manuscript, which greatly improved the final MS. Thanks are extended to Robert F. Martin and Andrew M. McDonald for their final corrections. This research has been financially supported by the Spanish project CGL2007–61205 of the MEC and PROMES–RESRO1 of the BRGM, France, the research group (RNM 131) of the Junta de Andalucía, and F.P.I grant BES–2005–8328 of the Spanish Ministry of Education and Sciences. The analytical data from GEMOC were obtained using instrumentation funded by DEST Systemic Infrastructure Grants, ARC LIEF, NCRIS, industry partners and Macquarie University. This is contribution 1 from the ARC Centre of Excellence for Core to Crust Fluid Systems (http://www.ccfs.mq.edu.au) and 724 in the GEMOC Key Centre (http://www.gemoc.mq.edu.au).

References

Aitchison, J., Clarke, G. L., Meffre, S. & Cluzel, D. (1995): Eocene arc – continental collision in New Caledonia and implications for regional southwest Pacific tectonic evolution. *Geology* **23**, 161-164.

Alt, J.C. & Shanks, W.C. (1998): Serpentinization of abyssal peridotites from the MARK area, Mid-Atlantic Ridge: sulfur geochemistry and reaction modeling. *Geochim. Cosmochim. Acta* **76**, 641-653.

Andrews, D.R.A. & Brenan, J.M. (2002): Phase-equilibrium constraints on the magmatic origin of laurite + Ru–Os–Ir alloy. *Can. Mineral.* **40**, 1705-1716.

Arai, S. (1992): Chemistry of chromian spinel in volcanic rocks as a potential guide to magma chemistry. *Mineral. Mag.* **56**, 173-184.

Augé, T. (1988): Platinum-group-minerals in the Tiébaghi and Vourinos ophiolite complex: genetic implications. *Can. Mineral.* **26**, 177-192.

Augé, T., Genna, A., Legendre, O., Ivanov, K.S. & Volchenko, Y.A. (2005): Primary platinum mineralization in the Nizhny Tagil and Kachkanar ultramafic complexes, Urals, Russia: a genetic model for PGE concentration in chromite-rich zones. *Econ. Geol.* **100**, 707-732.

Augé, T. & Johan, Z. (1988): Comparative study of chromite deposits from Troodos, Vourinos, North Oman and New Caledonia ophiolites. *In* Mineral Deposits within the European Comunity (J. Boissonnas & P. Omenetto, eds.). *Soc. For Geology Applied to Mineral Deposits, Spec. Publ.* **6**, 167-288.

Augé, T. & Legendre, O. (1994): Platinum-group element oxides from the Pirogues ophiolitic mineralization, New Caledonia: origin and significance. *Econ. Geol.* **89**, 1454-1468.

Augé, T., Legendre, O. & Maurizot, P. (1998): The distribution of Pt and Ru–Os–Ir minerals in the New Caledonia Ophiolite. *In* International Platinum (N.P. Laverov & V.V. Distler, eds.). Theophrastus Publications, St. Petersburg, Russia (141-154).

Augé, T. & Maurizot, P. (1995): Stratiform and alluvial platinum mineralization in the New Caledonia ophiolite complex. *Can. Mineral.* **33**, 1023-1045.

Auzende, J.-M., Van De Beuque, S., Réginier, M., Lafoy, Y. & Symonds, P. (2000): Origin of the New Caledonian ophiolites based on a French–Australian seismic transect. *Mar. Geol.* **162**, 225-236.

Ballhaus, C., Bockrath, C., Wohlegemuth-Uberwasser, C., Laurenz, V. & Berndt, J. (2006): Fractionation of the noble metals by physical processes. *Contrib. Mineral. Petrol.* **152**, 667-684.

Ballhaus, C.G. & Stumpfl, E.F. (1986): Sulfide and platinum mineralization in the Merensky Reef: evidence from hydrous silicates and fluids inclusions. *Contrib. Mineral. Petrol.* **94**, 193-204.

Ballhaus, C., Tredoux, M. & Späth, A. (2001): Phase relations in the Fe–Ni–Cu–PGE–S system at magmatic temperature and application to massive sulphide ores of the Sudbury igneous complex. *J. Petrol.* **42**, 1911-1926.

Barin, I. (1995): *Thermochemical Data of Pure Substances* (third ed.). VCH, Weinheim, Germany.

Barnes, S.J. & Roeder, P.L. (2001): The range of spinel compositions in terrestrial mafic and ultramafic rocks. *J. Petrol.* **42**, 2279-2302.

Bockrath, C., Ballhaus, C. & Holzheid, A. (2004): Stabilities of laurite RuS_2 and monosulfide liquid solution at magmatic temperature. *Chem. Geol.* **208**, 265-271.

Brenan, J.M. & Andrews, D.R.A. (2001): High-temperature stability of laurite and Ru–Os–Ir alloys and their role in PGE fractionation in mafic magmas. *Can. Mineral.* **39**, 341-360.

Carmichael, I.S.E. (1967): The iron–titanium oxides of salic volcanic rocks and their associated ferromagnesian silicates. *Contrib. Mineral. Petrol.* **14**, 36-64.

Cluzel, D., Aitchison, J., Clarke, G., Meffre, S. & Picard, C. (1994): Point de vue sur l'évolution tectonique et géodynamique de la Nouvelle-Calédonie (Pacifique). *C.R. Acad. Sci. Paris* **319**, *Sér. II*, 683-688.

Cluzel, D., Aitchison, J., Clarke, G., Meffre, S. & Picard, C. (1995): Dénudation tectonique du complexe à noyau métamorphique de haute pression tertiaire (nord de la

Nouvelle-Calédonie, Pacifique, France). *C.R. Acad. Sci. Paris* **321,** *Sér. II*, 57-64.

Cluzel, D., Aitchison, J.C. & Picard, C. (2001): Tectonic accretion and underplating of mafic terranes in the Late Eocene intraoceanic fore-arc of New Caledonia (southwest Pacific): geodynamic implications. *Tectonophysics* **340**, 23-59.

Cluzel, D., Bosch, D., Paquette, J.-L., Lemennicier, Y., Montjoie, P. & Ménot, R.-P. (2005): Late Oligocene post-obduction granitoids of New Caledonia: a case for reactivated subduction and slab break-off. *Island Arc* **14**, 254-271.

Cluzel, D., Chiron, D. & Courme, D. (1998): Discordance de l'Eocène supérieur et événements pré-obduction of Nouvelle-Calédonie (Pacifique sud-ouest). *C.R. Acad. Sci. Paris* **327**, *Sér. II*, 485-491.

Collot, J.-Y., Malahoff, A., Récy, J., Latham, G. & Missègue, F. (1987): Overthurst emplacement of New Caledonia ophiolite: geophysical evidence. *Tectonics* **6**, 215-232.

Crawford, A.J., Meffre, S. & Symonds, P.A. (2003): 120–0 Ma tectonic evolution of the southwest Pacific and analogous geological evolution of the 600–220 Ma Tasman fold belt system. *Geol. Soc. Am., Spec. Pap.* **372**, 383-403.

Dare, S.A.S., Pearce, J.A., McDonald, I. & Styles, M.T. (2009): Tectonic discrimination of peridotites using fO_2–Cr# and Ga–Ti–Fe^{III} systematics in chrome-spinel. *Chem. Geol.* **261**, 199-216.

Dupuy, C., Dostal, J. & Leblanc, M. (1981): Geochemistry of an ophiolitic complex from New Caledonia. *Contrib. Mineral. Petrol.* **76**, 77-83.

Eckstrand, O.R. (1975): The Dumont serpentinite: a model for control of nickeliferous opaque minerals assemblages by alteration reactions in ultramafic rocks. *Econ. Geol.* **70**, 183-201.

El Ghorfi, M., Melcher, F., Oberthür, T., Boukhari, A.E., Maacha, L., Maddi, A. & Mhaili, M. (2008): Platinum group minerals in podiform chromitites of the Bou Azzer ophiolite, Anti Atlas, Central Morocco. *Mineral. Petrol.* **92**, 59-80.

Ferrario, A. & Garuti, G. (1990): Platinum-group mineral inclusions in chromitites of the Finero mafic-ultramafic complex (Ivrea-Zone, Italy). *Mineral. Petrol.* **41**, 125-143.

Garuti, G., Proenza, J.A. & Zaccarini, F. (2007): Distribution and mineralogy of platinum-group elements in altered chromitites of the Campo Formoso layered intrusion (Bahia State, Brazil): control by magmatic and hydrothermal processes. *Mineral. Petrol.* **89**, 159-188.

Garuti, G. & Zaccarini, F. (1997): In situ alteration of platinum-group minerals at low temperature: evidence from serpentinized and weathered chromitite of the Vourinos complex, Greece. *Can. Mineral.* **35**, 611-626.

Garuti, G., Zaccarini, F., Cabella, R. & Fershtater, G. (1997): Occurrence of an unknown Ru–Os–Ir–Fe oxides in the chromitites of the Nurali ultramafic complex, southern Urals, Russia. *Can. Mineral.* **35**, 1431-1439.

Garuti, G., Zaccarini, F., Moloshag, V. & Alimov, V. (1999): Platinum-group minerals as indicators of sulfur fugacity in ophiolite upper mantle: an example from chromitites of the Ray–Iz ultramafic complex, Polar Urals, Russia. *Can. Mineral.* **37**, 1099-1115.

Gervilla, F., Proenza, J.A., Frei, R., González-Jiménez, J.M., Garrido, C.J., Melgarejo, J.C., Meibom, A., Díaz-Martínez, R. & Lavaut, W. (2005): Distribution of platinum-group elements and Os isotopes in chromite ores from Mayarí–Baracoa ophiolite belt (eastern Cuba). *Contrib. Mineral. Petrol.* **150**, 589-607.

González-Jiménez, J.M., Gervilla, F., Proenza, J.A., Kerestedjian, T., Augé, T. & Bailly, L. (2009a): Zoning of laurite (RuS_2) – erlichmanite (OsS_2): implications for the genesis of PGM in ophiolite chromitites. *Eur. J. Mineral.* **21**, 419-432.

González-Jiménez, J.M., Kerestedjian, T., Proenza, J.A. & Gervilla, F. (2009b): Metamorphism on chromite ores from the Dobromirtsi ultramafic massif, Rhodope Mountains (SE Bulgaria). *Geol. Acta* **7**, 413-429.

González-Jiménez, J.M., Proenza, J.A., Gervilla, F., Melgarejo, J.C., Blanco-Moreno, J.A. Ruiz-Sánchez, R. & Griffin, W.L. (2011): High-Cr and high-Al chromitites from the Sagua de Tánamo district, Mayarí–Cristal ophiolitic massif (eastern Cuba): constraints on their origin from mineralogy and geochemistry of chromian spinel and platinum-group elements. *Lithos* **125**, 101-121.

Hattori, K.H., Takahashi, Y. & Augé, T. (2010): Mineralogy and origin of oxygen-bearing platinum–iron grains based on an X-ray absorption spectroscopy study. *Am. Mineral.* **95**, 622-630.

Holzheid, A. (2010): Separation of sulfide melt droplets in sulfur saturated liquids. *Chem. Geol.* **274**, 127-135.

Johan, Z. & Augé, T. (1986): Ophiolitic mantle sequences and their evolution: mineral chemistry constraints. *In* Metallogeny of the Basic and Ultrabasic Rocks (M.J. Gallagher, R.A. Ixer, C.R. Neary & H.M. Prichard, eds.). Institute of Mining and Metallurgy, London, U.K. (305-317).

Kelemen, P.B. (1990): Reaction between ultramafic wall rock and fractionating basaltic magma. I. Phase relations, the origin of calc-alkaline magma series, and the formation of discordant dunite. *J. Petrol.* **31**, 51-98.

Kelemen, P.B., Dick, H.J.B. & Quick, J.E. (1992): Formation of harzburgite by pervasive melt/rock reaction in the upper mantle. *Nature* **358**, 635-641.

Kelemen, P.B., Shimizu, N. & Salters, W.J.W. (1995): Extraction of mid-ocean ridge basalts from the upwelling mantle by focused flow of melt in dunite channels. *Nature* **375**, 747-753.

KLEIN, F. & BACH, W. (2009): Fe–Ni–Co–O–S phase relations in peridotite–seawater interactions. *J. Petrol.* **50**, 37-59.

KRSTIC, S. & TARKIAN, M. (1997): Platinum-group minerals in gold-bearing placers associated with the Veluce ophiolite complex, Yugoslavia. *Can. Mineral.* **35**, 1-21.

LEGENDRE, O. & AUGÉ, T. (1986): Mineralogy of platinum group mineral inclusion in chromitites from different ophilitic complexes. *In* Metallogeny of the Basic and Ultrabasic Rocks (M.J. Gallagher, R.A. Ixer, C.R. Neary & H.M. Prichard, eds.). Institute of Mining and Metallurgy, London, U.K. (361-372).

LOCMELIS, M., MELCHER, F. & OBERTHÜR, T. (2010): Platinum-group element distribution in the oxidized Main Sulfide zone, Great Dyke, Zimbabwe. *Mineral. Deposita* **45**, 93-109.

LORAND, J.-P., ALARD, O. & LUGUET, A. (2010): Platinum-group element micronuggets and refertilization process in Lherz orogenic peridotite (northeastern Pyrenees, France). *Earth Planet. Sci. Lett.* **289**, 298-310.

MAJZLAN, J., MAKOVICKY, M., MAKOVICKY, E. & ROSE-HANSEN, J. (2002): The system Fe–Pt–S at 1100°C. *Can. Mineral.* **40**, 509-517.

MAKOVICKY, E. & KARUP-MØLLER, S. (2000): Phase relations in the metal-rich portions of the phase system Pt–Ir–Fe–S at 1000°C and 1100°C. *Mineral. Mag.* **63**, 379-385.

MAKOVICKY, M., MAKOVICKY, E. & ROSE-HANSEN, J. (1986): Experimental studies on the solubility and distribution of platinum group elements in base metal sulfides in platinum deposits. *In* Metallogeny of Basic and Ultrabasic Rocks (M.J. Gallagher, R.A. Ixer, C.R. Neary & H.M. Prichard, eds.). Institution of Mining and Metallurgy, London, U.K. (415-425).

MALITCH, K.N., THALHAMMER, O.A.R. KNAUF, V.V. & MELCHER, F. (2003): Diversity of platinum-group mineral assemblages in banded and podiform chromitite from Kraubath ultramafic massif, Austria: evidence for an ophiolitic transition zone. *Mineral. Deposita* **38**, 282-297.

MALLMANN, G. & O'NEILL, H.ST.C. (2009): The crystal/melt partitioning of V during mantle melting as function of oxygen fugacity compared with some other elements (Al, P, Ca, Sc, Ti, Cr, Fe, Ga, Y, Zr and Nb). *J. Petrol.* **50**, 1765-1794.

MARCHESI, C., GARRIDO, C.J., GODARD, M., BELLEY, F. & FERRÉ, E. (2009): Migration and accumulation of ultra-depleted subduction-related melts in the Massif du Sud ophiolite (New Caledonia). *Chem. Geol.* **266**, 171-186.

MATVEEV, S. & BALLHAUS, C. (2002): Role of water in the origin of podiform chromitite deposits. *Earth Planet. Sci. Lett.* **203**, 235-243.

MCKENZIE, D. (1989): Some remarks on the movement of small melt fractions in the mantle. *Earth Planet. Sci. Lett.* **95**, 53-72.

MELCHER, F., GRUM, W., SIMON, G., THALHAMMER, T.V. & STUMPFL, E.F. (1997): Petrogenesis of the ophiolitic giant chromite deposits of Kempirsai, Kazakhstan: a study of solid and fluid inclusions in chromite. *J. Petrol.* **38**, 1419-1458.

MORENO, T., PRICHARD, H.M., LUNAR, R., MONTERRUBIO, S. & FISHER, P. (1999): Formation of a secondary platinum-group mineral assemblage in chromitites from the Herbeira ultramafic massif in Cabo Ortegal, NW Spain. *Eur. J. Mineral.* **11**, 363-378.

MOUTTE, J. (1982): Chromite deposits of the Tiébaghi ultramafic massif, New Caledonia. *Econ. Geol.* **77**, 576-591.

NICOLAS, A. & PRINZHOFER, A. (1983): Cumulative or residual origin for the transition zone in ophiolites: structural evidence. *J. Petrol.* **24**, 188-206.

PAGÉ, P. & BARNES, S.-J. (2009): Using trace elements in chromites to constrain the origin of podiform chromitites in the Thetford Mines ophiolite, Québec, Canada. *Econ. Geol.* **104**, 997-1018.

PARKINSON, I.J. & ARCULUS, R.J. (1999): The redox state of subduction zones: insights from arc-peridotites. *Chem. Geol.* **160**, 409-423.

PRICHARD, H.M & LORD, R.A. (1994): Evidence for the mobility of PGE in the secondary environment in the Shetland ophiolite complex. *Trans. Inst. Mining. Metall., Sect. B.* **103**, 79-86.

PRICHARD, H.M., NEARY, C.R., FISHER, F.C. & O'HARA, M.J. (2008): PGE-rich podiform chromitites in the Al'Ays ophiolite complex, Saudi Arabia: an example of critical mantle melting to extract and concentrate PGE. *Econ. Geol.* **103**, 1507-1529.

PRINZHOFER, A. (1981): *Structure et pétrologie d'un cortège ophiolitique: le massif du Sud (Nouvelle-Calédonie).* Ph.D. thesis, Ecole Normale Supérieure Des Mines, Paris, France.

PRINZHOFER, A. & ALLÈGRE, C.J. (1985). Residual peridotites and the mechanisms of partial melting. *Earth Planet. Sci. Lett.* **74**, 251-265.

PRINZHOFER, A., NICOLAS, A., CASSARD, D., MOUTTE, J., LEBLANC, M., PARIS, J.P. & RABINOVITCH, M. (1980): Structures in the New Caledonia peridotites–gabbros: implications for oceanic mantle and crust. *Tectonophysics* **69**, 85-112.

PROENZA, J.A., ZACCARINI, F., CÁBANA, C., ESCAYOLA, M., SHALAMUK, A. & GARUTI, G. (2008): Chromite composition and platinum-group minerals in chromitites of the western ophiolitic belt from Pampeans Ranges of Córdoba, Argentina. *Ore Geol. Rev.* **33**, 32-48.

PROENZA, J.A., ZACCARINI, F., LEWIS, J.F., LONGO, F. & GARUTI, G. (2007): Chromian spinel composition and the platinum-group minerals of the PGE-rich Loma Peguera

chromitites, Loma Caribe peridotite, Dominican Republic. *Can. Mineral.* **45**, 631-648.

ROEDER, P.L. & JAMIESON, H.E. (1992): Composition of chromite and co-existing Pt–Fe alloy at magmatic temperatures. *Aust. J. Earth. Sci.* **39**, 419-426.

SINGH, A.K. & SINGH, R.K. (2011): Zn- and Mn-rich chromespinels in serpentinite in Tidding Suture Zone, eastern Himalaya and their metamorphism and genetic significance. *Current Science* **100**, 743-749.

SPANDLER, C., RUBATTO, D. & HERMANN, J. (2005): Late Cretaceous – Tertiary tectonics of the southwest Paficic: insights from U–Pb sensitive, high-resolution ion microprobe (SHRIMP) dating of eclogite facies rocks from New Caledonia. *Tectonics* **24**, TC3003, doi: 10.029/2004TC001709.

STOCKMAN, H.W. & HLAVA, P.F. (1984): Platinum-group minerals in Alpine chromitites from southwestern Oregon. *Econ. Geol.* **79**, 491-508.

SUAREZ, S., PRICHARD, H.M., VELASCO, F., FISHER, P.C. & MCDONALD, I. (2010): Alteration of platinum-group minerals and dispersion of platinum-group elements during progressive weathering of the Aguablanca Ni–Cu deposit, SW Spain. *Mineral. Deposita* **45**, 331-350.

THALHAMMER, O.A.R., PROCHASKA, W. & MÜHLHANS, H.W. (1990): Solid inclusions in chrome-spinels and platinum group element concentrations from the Hochgrössen and Kraubath ultramafic massif (Austria). *Contrib. Mineral. Petrol.* **105**, 66-80.

TSOUPAS, G. & ECONOMOU-ELIOPOULOS, M. (2008): High PGE contents and extremely abundant PGE-minerals hosted in chromitites from the Veria ophiolite complex, northern Greece. *Ore Geol. Rev.* **33**, 3-19.

UYSAL, I., ZACCARINI, F., SAKILAR, B., TARKIAN, M., BERNHARD, H.-J., BIGI, S. & GARUTI, G. (2009): Occurrence of rare Ru–Fe–Os–Ir-oxide and associated platinum-group minerals (PGM) in the chromitite of Muğla ophiolite, SW-Turkey. *Neues Jahrb. Mineral., Abh.* **185**, 323-333.

YANG, KAI & SECCOMBE, P.K. (1993): Platinum-group minerals in the chromitites from the Great Serpentinite Belt, NSW, Australia. *Mineral. Petrol.* **47**, 263-286.

ZACCARINI, F., PROENZA, J.A., RUDASHEVSKY, N.S., CABRI, L.J., GARUTI, G., RUDASHEVSKY, V.N., MELGAREJO, J.C., LEWIS, J.F., LONGO, F., BAKKER, R.J. & STANLEY, C.J. (2009): The Loma Peguera ophiolitic chromitite (central Dominican Republic): a source of new platinum group minerals (PGM) species. *Neues Jahrb. Mineral., Abh.* **185**, 335-349.